AGU PUBLICATIONS

Global Biogeochemical Cycles

RESEARCH ARTICLE
10.1002/2017GB005790

Key Points:
- Tidal wetlands, estuaries, and shelf waters each contribute substantially to the carbon budget of eastern North American coastal waters
- Study region net ecosystem production, atmospheric uptake, and burial are 20.2 ± 4.4, 5.1 ± 2.4, and 2.5 ± 0.7 Tg C yr^{-1}, respectively
- Net lateral carbon fluxes between tidal wetlands, estuaries, and shelf waters are large terms in the carbon budget of eastern North American coastal waters

Supporting Information:
- Supporting Information S1
- Data Set S1
- Table S1
- Table S2

Correspondence to:
R. G. Najjar,
rgn1@psu.edu

Citation:
Najjar, R. G., Herrmann, M., Alexander, R., Boyer, E. W., Burdige, D. J., Butman, D., et al (2018). Carbon budget of tidal wetlands, estuaries, and shelf waters of eastern North America. *Global Biogeochemical Cycles*, *32*, 389–416. https://doi.org/10.1002/2017GB005790

Received 25 AUG 2017
Accepted 14 FEB 2018
Accepted article online 20 FEB 2018
Published online 11 MAR 2018
Corrected 4 APR 2018

This article was corrected on 4 APR 2018. See the end of the full text for details.

Carbon Budget of Tidal Wetlands, Estuaries, and Shelf Waters of Eastern North America

R. G. Najjar[1], M. Herrmann[1], R. Alexander[2], E. W. Boyer[3], D. J. Burdige[4], D. Butman[5], W.-J. Cai[6], E. A. Canuel[7], R. F. Chen[8], M. A. M. Friedrichs[7], R. A. Feagin[9], P. C. Griffith[10], A. L. Hinson[9], J. R. Holmquist[11], X. Hu[12], W. M. Kemp[13], K. D. Kroeger[14], A. Mannino[15], S. L. McCallister[16], W. R. McGillis[17], M. R. Mulholland[4], C. H. Pilskaln[18], J. Salisbury[19], S. R. Signorini[15], P. St-Laurent[7], H. Tian[20], M. Tzortziou[21,17], P. Vlahos[22], Z. A. Wang[23], and R. C. Zimmerman[4]

[1]Department of Meteorology and Atmospheric Science, The Pennsylvania State University, University Park, PA, USA, [2]U. S. Geological Survey, National Center, Reston, VA, USA, [3]Department of Ecosystem Science and Management, The Pennsylvania State University, University Park, PA, USA, [4]Department of Ocean, Earth, and Atmospheric Sciences, Old Dominion University, Norfolk, VA, USA, [5]Department of Civil and Environmental Engineering, University of Washington, Seattle, WA, USA, [6]College of Earth, Ocean, and the Environment, University of Delaware, Newark, DE, USA, [7]Virginia Institute of Marine Science, College of William & Mary, Gloucester Point, VA, USA, [8]School for the Environment, University of Massachusetts Boston, Boston, MA, USA, [9]Department of Ecosystem Science and Management, Texas A&M University, College Station, TX, USA, [10]Carbon Cycle and Ecosystems Office, NASA Goddard Space Flight Center, Greenbelt, MD, USA, [11]Smithsonian Environmental Research Center, Edgewater, MD, USA, [12]Department of Physical and Environmental Sciences, Texas A&M University-Corpus Christi, Corpus Christi, TX, USA, [13]Horn Point Laboratory, University of Maryland Center for Environmental Science, Cambridge, MD, USA, [14]U. S. Geological Survey, Woods Hole Coastal and Marine Science Center, Woods Hole, MA, USA, [15]Ocean Ecology Laboratory, NASA Goddard Space Flight Center, Greenbelt, MD, USA, [16]Department of Biology, Virginia Commonwealth University, Richmond, VA, USA, [17]Lamont-Doherty Earth Observatory, Columbia University, Palisades, NY, USA, [18]Department of Estuarine and Ocean Sciences, School for Marine Science and Technology, University of Massachusetts Dartmouth, New Bedford, MA, USA, [19]School of Marine Science and Engineering, University of New Hampshire, Durham, NH, USA, [20]School of Forestry and Wildlife, Auburn University, Auburn, AL, USA, [21]Department of Earth and Atmospheric Science, The City College of New York, New York, NY, USA, [22]Department of Marine Science, University of Connecticut, Storrs, CT, USA, [23]Department of Marine Chemistry and Geochemistry, Woods Hole Oceanographic Institution, Woods Hole, MA, USA

Abstract Carbon cycling in the coastal zone affects global carbon budgets and is critical for understanding the urgent issues of hypoxia, acidification, and tidal wetland loss. However, there are no regional carbon budgets spanning the three main ecosystems in coastal waters: tidal wetlands, estuaries, and shelf waters. Here we construct such a budget for eastern North America using historical data, empirical models, remote sensing algorithms, and process-based models. Considering the net fluxes of total carbon at the domain boundaries, 59 ± 12% (± 2 standard errors) of the carbon entering is from rivers and 41 ± 12% is from the atmosphere, while 80 ± 9% of the carbon leaving is exported to the open ocean and 20 ± 9% is buried. Net lateral carbon transfers between the three main ecosystem types are comparable to fluxes at the domain boundaries. Each ecosystem type contributes substantially to exchange with the atmosphere, with CO_2 uptake split evenly between tidal wetlands and shelf waters, and estuarine CO_2 outgassing offsetting half of the uptake. Similarly, burial is about equal in tidal wetlands and shelf waters, while estuaries play a smaller but still substantial role. The importance of tidal wetlands and estuaries in the overall budget is remarkable given that they, respectively, make up only 2.4 and 8.9% of the study domain area. This study shows that coastal carbon budgets should explicitly include tidal wetlands, estuaries, shelf waters, and the linkages between them; ignoring any of them may produce a biased picture of coastal carbon cycling.

Plain Language Summary A carbon budget for a particular site or region describes the inputs and outputs of carbon to that site or region as well as the processes that change carbon from one form to another. A carbon budget is needed to fully understand many important issues facing coastal waters. We constructed the carbon budget for coastal waters of eastern North America. We found that about 60% of the carbon entering the domain is from rivers and about 40% is from the atmosphere, while about 80% of the carbon leaving the domain goes to the open ocean and about 20% is buried. Transfers of carbon from wetlands to estuaries and from estuaries to the ocean were as important as transfers of carbon at the domain boundaries. Tidal wetlands and estuaries were found to be important to the carbon budget despite making up only 2.4 and 8.9% of the study domain area, respectively. This study shows that coastal carbon budgets should explicitly consider tidal wetlands,

estuaries, shelf waters, and the linkages between them; ignoring any of them may produce a biased picture of coastal carbon cycling.

1. Introduction

The coastal zone, which includes the continuum of tidal wetlands, estuaries, and continental shelf waters, occupies a small fraction of the Earth's surface but plays a significant role in the global carbon cycle. For example, according to current global estimates, tidal wetlands account for about a third of the ocean's total carbon burial (Duarte et al., 2005); the net CO_2 degassing by estuaries is between 0.1 and 0.4 Pg C yr^{-1}, as much as one quarter of the net uptake of atmospheric CO_2 by the open ocean (Borges & Abril, 2011; Borges et al., 2005; Cai, 2011; Chen et al., 2013); and primary production in continental shelf waters is 10–30% of the ocean's total, despite making up only 7–10% of the ocean's area (Bauer et al., 2013).

An understanding of carbon cycling in the coastal zone has benefits that extend beyond the global carbon cycle. Because carbon is a common currency for describing many ecological and geochemical phenomena, the articulation of a carbon budget can enhance the understanding of numerous critical issues in the coastal zone, including hypoxia, which is driven by the oxidation of organic carbon (Diaz & Rosenberg, 2008); acidification, which results from the invasion of anthropogenic CO_2 and organic carbon oxidation (Cai et al., 2011); and the loss of carbon sequestration potential (blue carbon) through human development and sea level rise (Pendleton et al., 2012). Defining and balancing the carbon budget takes on some urgency due to rapid coastal development, accelerating climate change, and the need to better quantify the role of coastal ecosystems as sources and sinks of carbon.

At the global scale, progress has been made in recent years in creating coastal zone carbon budgets. Regnier et al. (2013) made global estimates for riverine input, tidal wetland exchange with estuaries, estuarine outgassing, estuarine burial, and exchange between estuaries and shelf waters. However, numerous terms in their budget are poorly constrained, an example being exchange between tidal wetlands and estuaries, which is based on data from one region. Furthermore, Regnier et al. (2013) ignore shelf waters and transformations between organic and inorganic carbon. Bauer et al. (2013) included shelf waters in their global budget but concluded that riverine input is the only major term for which there is 95% certainty that the estimate is within 50% of the reported value. Hence, major gaps remain in coastal carbon budgets at the global scale.

At the regional scale, coastal carbon budgets are scarce; we are aware of only three peer-reviewed coastal carbon budgets for large stretches of coastline (>1,000 km), all of which are focused on estuaries. Herrmann et al. (2015) constructed an organic carbon budget for 52 estuaries of the eastern United States using empirical models. Mechanistic modeling was applied to construct inorganic and organic carbon budgets to most of these estuaries by Laruelle et al. (2017), with very few field data for model calibration, and to six estuaries of the North Sea by Volta et al. (2016). These studies highlight the important but spatially variable role that estuaries play in processing carbon from rivers and tidal wetlands before it reaches shelf waters.

The Ocean Carbon and Biogeochemistry Program and the North American Carbon Program began promoting carbon cycle research and synthesis in the coastal zone with a workshop in 2005 focused on North American coastal margins. The report from that workshop (Hales et al., 2008) recommended synthesis of data relevant to North American coastal carbon cycling and the development of regional carbon budgets for the continent's main coastal regions. Following this recommendation and similar recommendations of Doney et al. (2004) and Chavez et al. (2007), the National Aeronautics and Space Administration supported funding for regional workshops and initial data synthesis, which led to the development of preliminary coastal carbon budgets for North America (Alin et al., 2012; Coble et al., 2010; Mathis & Bates, 2010; McKinley et al., 2011; Najjar et al., 2012). With the exception of riverine delivery of carbon to coastal waters of the contiguous United States (Shih et al., 2010; Stets & Striegl, 2012), large uncertainties were identified in the regional carbon budgets. A major outcome of the North American regional carbon budget assessment was the realization that the great spatial and temporal heterogeneity of coastal systems demands novel techniques for extrapolating limited in situ data on carbon fluxes to greater spatial and temporal scales. Remote sensing, statistical approaches, and process-based numerical models were identified as key resources.

The present study is a direct outcome of the workshop on Eastern North America (ENA; Najjar et al., 2012) and research that was presented at or initiated by the workshop, including studies on the air-sea CO_2 flux for shelf

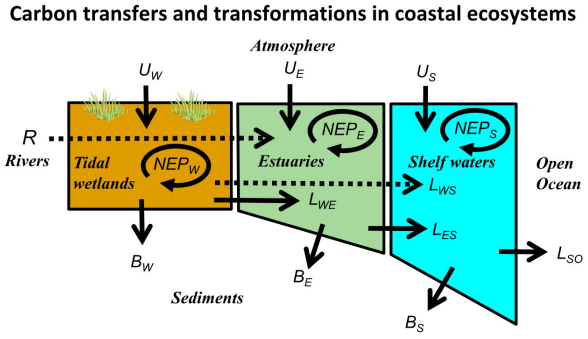

Figure 1. Conceptual diagram for the carbon balance of coastal ecosystems. The relevant fluxes are uptake of atmospheric CO_2 (U), burial of organic carbon (B), riverine input (R), and lateral transport (L). Subscripts W, E, S, and O represent tidal wetlands, estuaries, shelf waters, and the open ocean, respectively. Dashed arrows represent carbon pathways not directly passing through either tidal wetlands or estuaries. NEP = net ecosystem production.

waters (Signorini et al., 2013), the estuarine organic carbon balance (Herrmann et al., 2015), and riverine input (Tian et al., 2015). Our main objective is to develop the first complete carbon budget for ENA coastal waters. To our knowledge, this is the first attempt at developing a budget for a large coastline from the head of tide to the continental shelf. Some research questions that can be addressed with such a budget include the following: (1) Does any ecosystem type (tidal wetlands, estuaries, or shelf waters) dominate any aspect of the budget? (2) What are the major sources and sinks of carbon for the study domain? (3) Is the study domain as a whole a source or sink of atmospheric CO_2? (4) How much carbon is buried in the study domain? (5) How important are lateral transfers between ecosystem types compared to other budget terms? and (6) What is the metabolic poise (net autotrophic or net heterotrophic) of the study domain?

2. Budget Framework

We sought to determine the carbon fluxes for three main ecosystems: tidal wetlands, estuarine open waters (without emergent vegetation, "estuaries" hereafter), and continental shelf waters. Each ecosystem has a boundary with the atmosphere and within the sediments (Figure 1). The sediment boundary was taken to be the depth below which permanent burial occurs. The landward boundary of tidal wetlands and estuaries was located at the head of tide, the estuary-wetland boundary was taken to be the mean position of the open-water edge, and the seaward boundary of continental shelf waters was located at approximately the 100 m isobath.

The relevant carbon fluxes explicitly resolved in our study at the boundaries of the ecosystems are the net uptake from the atmosphere by tidal wetlands (U_W), estuaries (U_E), and shelf waters (U_S); burial in tidal wetland soils (B_W), estuarine sediments (B_E), and continental shelf sediments (B_S); riverine input from land to estuaries (R); and the net lateral advective transports from ecosystem I to ecosystem J (L_{IJ}), including tidal wetlands to estuaries (L_{WE}), tidal wetlands to shelf waters (L_{WS}), estuaries to shelf waters (L_{ES}), and shelf waters to the open ocean (L_{SO}). Superscripts, when present (see below), indicate the form of carbon: organic (O), inorganic (I), or total (T). Total carbon fluxes are simply the sum of the organic and inorganic carbon fluxes (e.g., $R^T = R^O + R^I$). For consistency across domains, we adopt the convention of a flux from the atmosphere as being a positive number, even though atmospheric scientists and oceanographers often use the opposite sign convention.

Internal transformations in tidal wetlands, estuaries, and shelf waters are net primary production (NPP) and heterotrophic respiration (HR). Net ecosystem production (NEP), which represents the net internal transformation from inorganic carbon to organic carbon (Chapin et al., 2006; Hopkinson & Smith, 2005) is defined as

$$\mathrm{NEP} = \mathrm{NPP} - \mathrm{HR}. \quad (1)$$

Positive and negative NEP, respectively, indicate net autotrophy and net heterotrophy.

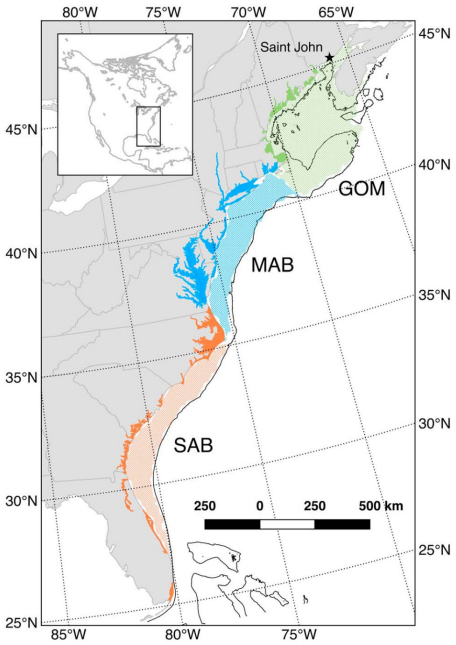

Figure 2. Study domain indicating locations of estuaries (darker colors) and shelf waters (lighter shading) in the three subregions: the Gulf of Maine (GOM), the Mid-Atlantic Bight (MAB), and the South Atlantic Bight (SAB). The 100 m isobath is shown as a solid black line. The outline of the St. John estuary in Canada was not available, so it is indicated by a star. Note that the northernmost SAB estuary, Albemarle Sound, appears to exchange with shelf waters of the MAB but actually exchanges with its neighbor to the south, Pamlico Sound, which exchanges with shelf waters of the SAB (Xie & Pietrafesa, 1999).

In our framework, we employ steady state mass balances of organic, inorganic, and total carbon for tidal wetlands, estuaries, and shelf waters:

$$\mathrm{NEP_W} = B_\mathrm{W} + L^\mathrm{O}_\mathrm{WE} + L^\mathrm{O}_\mathrm{WS} \quad (2a)$$

$$\mathrm{NEP_E} + L^\mathrm{O}_\mathrm{WE} + R^\mathrm{O} = B_\mathrm{E} + L^\mathrm{O}_\mathrm{ES} \quad (2b)$$

$$\mathrm{NEP_S} + L^\mathrm{O}_\mathrm{WS} + L^\mathrm{O}_\mathrm{ES} = B_\mathrm{S} + L^\mathrm{O}_\mathrm{SO} \quad (2c)$$

$$U_\mathrm{W} = \mathrm{NEP_W} + L^\mathrm{I}_\mathrm{WE} + L^\mathrm{I}_\mathrm{WS} \quad (3a)$$

$$U_\mathrm{E} + L^\mathrm{I}_\mathrm{WE} + R^\mathrm{I} = \mathrm{NEP_E} + L^\mathrm{I}_\mathrm{ES} \quad (3b)$$

$$U_\mathrm{S} + L^\mathrm{I}_\mathrm{WS} + L^\mathrm{I}_\mathrm{ES} = \mathrm{NEP_S} + L^\mathrm{I}_\mathrm{SO} \quad (3c)$$

$$U_\mathrm{W} = B_\mathrm{W} + L^\mathrm{T}_\mathrm{WE} + L^\mathrm{T}_\mathrm{WS} \quad (4a)$$

$$U_\mathrm{E} + L^\mathrm{T}_\mathrm{WE} + R^\mathrm{T} = B_\mathrm{E} + L^\mathrm{T}_\mathrm{ES} \quad (4b)$$

$$U_\mathrm{S} + L^\mathrm{T}_\mathrm{WS} + L^\mathrm{T}_\mathrm{ES} = B_\mathrm{S} + L^\mathrm{T}_\mathrm{SO}, \quad (4c)$$

where equations (2a)–(2c), (3a)–(3c), and (4a)–(4c) are for organic, inorganic, and total carbon, respectively, and equations equations (2a), (3a), and (4a); (2b), (3b), and (4b); and (2c), (3c), and (4c) are for tidal wetlands, estuaries, and shelf waters, respectively. Sources are to the left of the equal signs and sinks are to the right. The equations are not independent because the total carbon equations are simply the sums of the organic and inorganic carbon equations, but all three forms are useful when constructing budgets. The nine steady state mass balances represented by equations (2)–(4) are central to our approach.

3. Study Domain

The study domain (Figure 2) extends from the southern tip of the Scotian Peninsula (Canada) to the southern tip of Florida (USA). The domain was divided into three major subregions, which are, from north to south, the Gulf of Maine (GOM), the Mid-Atlantic Bight (MAB), and the South Atlantic Bight (SAB). The extents of these three coastal subregions were defined by Hofmann et al. (2011), and numerical values for the areas were provided by Signorini et al. (2013). The streamflow, number of estuaries, and areas of drainage basins, estuaries, seagrasses, tidal wetlands, and nonestuarine coastal waters ("shelf waters" hereafter) are provided in Table 1.

U.S. estuarine surface area was taken from Herrmann et al. (2015), whose primary sources were the National Oceanic and Atmospheric Administration's National Estuarine Eutrophication Assessment survey (Bricker et al., 2007) and a digital spatial framework based on a U.S. Geological Survey watershed hierarchy known as the Coastal Assessment Framework (NOAA, 1985). This framework makes a distinction between land areas draining into the estuaries (Estuarine Drainage Areas, EDAs) and those draining directly to shelf waters (Coastal Drainage Areas, CDAs). While the analysis of Herrmann et al. (2015) included only EDAs, the present study also includes the CDAs in the total watershed areas for each region.

There was no readily available estuarine inventory for the Canadian portion of the GOM. The St. John River (Figure 2) accounts for most of the streamflow entering the GOM at the Canadian coastline (McAdie, 1995) and is also the only river for which we could locate relevant information concerning carbon fluxes (Clair et al., 2013) and characteristics of its receiving estuary (Metcalfe et al., 1976). The next largest river, the St. Croix, has less than 10% of the flow of the St. John. Constructing individual carbon budgets for all Canadian GOM estuaries is thus not possible at this time, and so the only Canadian estuary explicitly included in our analysis is the St. John River estuary. To estimate the total contribution from Canadian estuaries to the carbon budget, we used a freshwater scaling factor of 0.59^{-1} (i.e., 1.69), where 0.59 is the proportion of the

Table 1
Characteristics of Subregions in the Study Domain

Region	Catchment area[a] (10^3 km^2)	Streamflow[b] (m^3 s^{-1})	No. of estuaries[c]	Tidal wetland area[d] (10^3 km^2)	Shelf tidal wetlands[e] (%)	Estuary area[f] (10^3 km^2)	Seagrass area[g] (10^3 km^2)	Shelf area[h] (10^3 km^2)
GOM	177	3458	>20	0.51 ± 0.27	25.0	5.7	0.26	186
MAB	297	4424	13	3.61 ± 0.72	8.9	20.3	0.84	93
SAB	331	3787	20	6.01 ± 0.92	17.0	12.2	0.85	102
ENA	805	11669	>53	10.13 ± 1.20	14.5	38.2	1.95	381

Note. GOM = Gulf of Maine; MAB = Mid-Atlantic Bight; SAB = South Atlantic Bight; ENA = Eastern North America.
[a]From Water Systems Analysis Group (2000) for the GOM and Herrmann et al. (2015) for the MAB and SAB. [b]From Herrmann et al. (2015), except for the Canadian portion of the GOM, which contributes the flow of the St. John, 1124 m^3 s^{-1} (Clair et al., 2013), times the freshwater scaling factor 1.69 (see text). [c]From Herrmann et al. (2015) except for the Canadian portion of the GOM, which increases the number by >1. [d]From Hinson et al. (2017) except for the Canadian portion of the GOM, which increases the area by 153 km^2 (Hanson & Calkins, 1996). Errors are based on Dahl (2011) (see text). [e]As a percent of total tidal wetland area. See text. [f]From Herrmann et al. (2015), except for the Canadian portion of the GOM, which contributes the area of the St. John River estuary, 244 km^2 (Metcalfe et al., 1976), times the freshwater scaling factor 1.69 (see text). [g]Seagrasses are assumed to be within estuaries only. GOM area is from Gustavson (2010). MAB area is the CEC (2016) "temperate North Atlantic" seagrass area (1,092 km^2, which includes the GOM, the MAB, and a small portion of the SAB) minus the GOM estimate. SAB area equals the eastern Florida seagrass area (333 km^2) from Yabro and Carlson (2011) plus prorated estimates for the remainder of the SAB using the NOAA (1975) tidal coastline lengths of 4,627, 3,771, and 5,376 km for South Carolina, Georgia, and eastern Florida, respectively. [h]From Signorini et al. (2013). Note that our definition of the GOM includes Georges Bank and Nantucket shoals.

total Canadian contribution of streamflow to the GOM originating from the St. John River only (McAdie, 1995). This scaling factor is then multiplied by several of the carbon fluxes for the St. John River estuary (section 4.2). This scaling factor was also used to estimate Canadian GOM estuarine area (Table 1).

U.S. tidal wetland areas were taken from Hinson et al. (2017), who distributed tidal wetland areas from the U.S. National Wetlands Inventory (Dahl & Stedman, 2013) among EDAs and CDAs. Four tidal wetland classes were considered: (1) emergent vegetation (equivalent to brackish to saline salt marsh), (2) shrub-scrub (equivalent to black mangroves in saline southern portions of the SAB but primarily several types of woody shrubs growing in brackish zones in the rest of the ENA study area), (3) forested (equivalent to taller red mangroves in the southern portion of the SAB and also small patches of nonmangrove woody species in the rest of the ENA study area), and (4) freshwater tidal (including all herbaceous, shrub, and forest vegetation in areas of no salinity); an example distribution of these wetlands and neighboring rivers, estuaries, and shelf waters is shown in Figure 3. ENA tidal wetlands are mostly emergent vegetation (73%) and freshwater tidal (21%), with the remainder (6%) being shrub-scrub and forested. We also distinguished between wetlands that drain to estuaries (i.e., wetlands located in an EDA) and wetlands that drain directly to shelf waters (i.e., wetlands located in a CDA). In the U.S. portion of the study area, 14.5% of the tidal wetland area drains directly to shelf waters. Canadian GOM tidal wetland area was taken from Hanson and Calkins (1996). Lacking knowledge of the location of Canadian tidal wetlands, we assumed that they all drain directly to the ocean.

The tidal wetland areas used here are an improvement over those used by Herrmann et al. (2015), which were based on wetlands delineated in the National Land Cover Database. Our estimates depart from those of this database by only −1% for ENA, but subregional departures are substantial: +27% for the GOM, +17% for the MAB, and −10% for the SAB. The GOM difference is primarily due to our inclusion of Canadian wetlands.

The subregions differ considerably in their physical characteristics (Table 1). About a quarter of the watershed of ENA drains to the GOM, and the remainder drains approximately evenly to the MAB and SAB. Nevertheless, runoff to each subregion is about the same, reflecting regional differences in precipitation and evapotranspiration. Estuarine surface area is 3.8 times the tidal wetland area and 20 times the seagrass area. More than half the estuarine surface area is in the MAB, a third is in the SAB, and less than a sixth is in the GOM. Thus, the MAB is the subregion most influenced by estuaries, particularly its large estuaries having long residence times, such as the Chesapeake Bay, Delaware Bay, and the Hudson River Estuary. The SAB, in contrast, contains more than half of the study area's tidal wetlands. Only 13% of ENA seagrass area is in the GOM, the remainder being split evenly between the MAB and SAB. Continental shelf waters make up 87% of the domain surface area, with about half the shelf water area in the GOM and the remainder split evenly between the MAB and SAB. An in-depth comparison of the shelf waters of the three subregions can be found in Jahnke et al. (2008) and Hofmann et al. (2008). Briefly, marine source waters for the study region are dominated by the Labrador Sea and Scotian Shelf to the north and the Gulf Stream to the south, which meet near the SAB/MAB boundary at Cape Hatteras. The GOM is semienclosed with several deep sub-basins and a

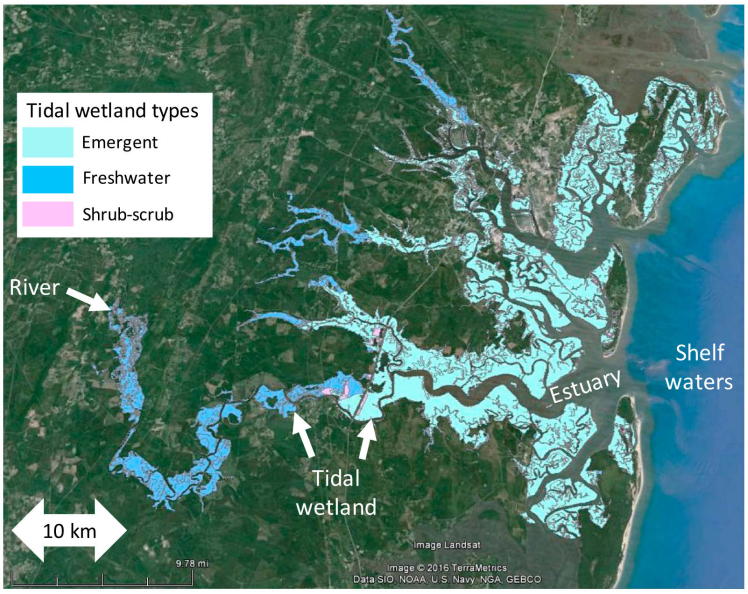

Figure 3. Example of the wetland class data set for St. Andrews/St. Simons Sounds, which is in the state of Georgia and part of the South Atlantic Bight subregion.

strong spring bloom. It also has strong winter mixing that allows respired CO_2 at depth to return to the atmosphere. The SAB is strongly influenced by Gulf Stream intrusions and filaments that generate blooms every few weeks.

4. Flux Estimation

A variety of approaches were used to estimate the terms in equations (2)–(4). Given the heterogeneity of the coastal zone and the scarcity of observations, we used, where possible, statistical models that are strongly constrained by observations in the study domain. Such was the case for riverine input of TOC (Shih et al., 2010), estuarine NEP and burial (Herrmann et al., 2015), and the exchange of CO_2 between shelf waters and the atmosphere (Signorini et al., 2013). Mechanistic models that have been extensively evaluated and calibrated were our second choice, and these were employed to quantify shelf water NEP (St-Laurent et al., 2017) and the riverine input of dissolved inorganic carbon (DIC) (Tian et al., 2015). Where regional, data-constrained models did not exist, we relied on simple averaging of the available data in the study domain; this approach was applied for NPP in all ecosystems, tidal wetland burial and lateral export, and the exchange of CO_2 between estuarine waters and the atmosphere. When regional models and data were not available, we used generic models, as in the case of burial in shelf sediments (Burdige, 2007). Finally, numerous fluxes were computed by difference using equations (2)–(4). Total carbon fluxes (equations (4a)–(4c)) were computed as sums of organic and inorganic carbon fluxes, except for exchange between shelf and open ocean waters, in which case the total carbon balance (equation (4c)) was used (see below). Additionally, HR was computed for each system using equation (1) and estimates of NPP and NEP.

Errors in flux per unit area were estimated using a variety of approaches. When possible, we used formal error estimates from data-constrained models. Fluxes based on data syntheses were assigned standard errors by taking the standard deviation of the mean. Interannual variability was used as a proxy for error for some

model-based fluxes. Finally, when error estimates were not possible using quantitative approaches, expert judgment was used.

Errors in domain area were estimated for tidal wetlands but not for estuaries and shelf waters. Estuaries and shelf waters are user defined, and hence, their areas have no errors. Dahl (2011) reported a standard error of 4.4% for the sum of emergent and shrub/scrub tidal wetland area of the contiguous United States. This error reflects the uncertainty in the methodology used to delineate the wetlands from surface imagery and to validate the delineations via field surveys. Unfortunately, error estimates are not available on local and regional scales, nor are they available for tidal freshwater wetlands. Therefore, to approximate errors on individual wetlands in our domain, we downscaled the aggregated fractional error reported by Dahl (2011), assuming that tidal wetland area errors are distributed evenly (i.e., wetlands that have equal areas also have equal errors), are uncorrelated (i.e., square of the aggregated error equals the sum of squared errors on the components), and add up to an aggregated fractional error of 4.4%, consistent with the fractional error reported by Dahl (2011). It follows that the standard error ε in any tidal wetland area A is given by

$$\varepsilon = \varepsilon_{\mathrm{US}} \sqrt{\frac{A}{A_{\mathrm{US}}}}, \tag{5}$$

where A_{US} is the area of estuarine wetlands in the contiguous United States (18,372 km^2) and $\varepsilon_{\mathrm{US}}$ is its standard error (808 km^2). Equation (5) was applied whenever any tidal wetland area was used in a flux calculation. Two standard errors in ENA tidal wetland area are equal to 12%, but subregional errors may be considerably larger (Table 1).

Standard error propagation techniques were used assuming uncorrelated errors when derived quantities were computed (Squires, 2001). In the end, best estimates and standard errors of all of the terms in equations (2)–(4) were made on a per unit area basis for each subregion and ENA as a whole. Whenever any quantity in this paper is presented as $X \pm Y$, X is the best estimate and Y is 2 standard errors, except where noted.

The entire system was assumed to be in steady state with respect to carbon dynamics over the past several decades, when most of the data for the analysis were collected. Hence, this study does not address seasonality and other forms of temporal variability, which are considerable for many of the fluxes.

4.1. Tidal Wetland Fluxes

4.1.1. Net Primary Production of Tidal Wetlands (NPP_W)

A synthesis of tidal wetland aboveground (or aerial) NPP and belowground NPP measurements in the United States was made by Continental Shelf Associates Inc. (1991, p. 91); the aboveground NPP synthesis is also presented in Mendelssohn and Morris (2000). We used the computed subregional averages and standard errors, which are based on 132 aboveground NPP estimates (18, 76, and 38 respectively from the GOM, MAB, and SAB) and 45 belowground NPP estimates (5, 29, and 11 respectively from the GOM, MAB, and SAB). Tidal wetland NPP is split evenly between aboveground and belowground in the GOM and SAB, whereas nearly ¾ of NPP is belowground in the MAB (Continental Shelf Associates Inc., 1991). We assumed that the U.S. GOM NPP estimates applied to all tidal wetlands of the GOM. Net primary production of tidal wetlands (NPP_W) was computed as the sum of aboveground and belowground NPP.

4.1.2. Burial in Tidal Wetlands (B_W)

Our estimates of tidal wetland burial in the study region are based on the global synthesis of carbon accumulation rate by Ouyang and Lee (2014), which contains 59 estimates in the study region (28, 23, and 8, respectively, from the GOM, MAB, and SAB). Carbon accumulation rate is the product of carbon density and sediment accumulation rate. For each subregion, we computed means and standard errors from these data.

4.1.3. Net Lateral Flux From Tidal Wetlands (L_{WE} and L_{WS})

The literature was synthesized to estimate the net lateral flux of total organic carbon (TOC = particulate organic carbon + dissolved organic carbon = POC + DOC) and DIC from tidal wetlands to estuaries and shelf waters. Twelve estimates of net TOC export (per unit area of wetland) were summarized in Herrmann et al. (2015), who found the mean to be 185 ± 71 g C m^{-2} yr^{-1}. We found four estimates of the net lateral DIC flux from tidal wetlands in ENA (Morris & Whiting, 1986; Neubauer & Anderson, 2003; Wang et al., 2016; Wang & Cai, 2004; Table S1 in the supporting information) and computed the mean to be 235 ± 120 g C m^{-2} yr^{-1}. We applied the computed means and standard errors of the net lateral TOC and DIC fluxes to all ENA tidal wetlands, independent of subregion. On a unit area basis, we assumed that the net flux of carbon from tidal wetlands to estuaries (L_{WE}) and shelf waters (L_{WS}) is the same.

4.1.4. Tidal Wetland Fluxes Computed as Residuals (NEP_W and U_W)

Assuming steady state, we computed NEP_W and U_W from equations (2a) and (4a), respectively. Our definition of U_W is the negative of tidal wetland net ecosystem exchange (Chapin et al., 2006).

4.1.5. Impact of Mangroves on Flux Estimates

Directly estimated tidal wetland fluxes (NPP_W, B_W, L_{WE}, and L_{WS}) are based on data from tidal marshes and assumed to apply to all tidal wetlands in the study domain. Mangroves make up, at most, 6% of the tidal wetland area in the domain (shrub-scrub and forested classes in Table 1). The global average NPP in mangroves has been estimated to be 33% larger than that in salt marshes (Alongi, 2014). Had we scaled shrub-scrub and forested wetlands to have an NPP 33% greater than that of salt marshes, then our integrated ENA tidal wetland NPP would increase by less than 2%. No correction would be necessary for burial because there is no significant difference between salt marshes and mangroves in terms of mean carbon burial (Alongi, 2014; Chmura et al., 2003; Ouyang & Lee, 2014). Finally, data on lateral fluxes from mangroves are extremely limited. Estimates by Ho et al. (2017) of the lateral flux from mangroves bordering the nearby Shark River, in southwestern Florida, range from 83 to 249 g C m^{-2} yr^{-1}, all less than our estimates. Applying the lower bound estimate to shrub-scrub and forested wetlands would decrease our integrated ENA tidal wetland lateral flux by less than 5%. In summary, while there are differences in carbon cycling between mangroves and marshes, these differences are too small to impact the ENA tidal wetland carbon budget.

4.2. Estuarine Fluxes

4.2.1. Estuarine Net Primary Production (NPP_E)

Estuarine NPP is assumed to be the sum of NPP from plankton and seagrass. We did not have enough information to include the potentially substantial contributions from macroalgae (Krause-Jensen & Duarte, 2016) and benthic algae (MacIntyre et al., 1996). Estimates of estuarine planktonic primary production were taken from the global synthesis of Cloern et al. (2014), which lists median annual production for 24 ENA estuaries (3, 15, and 6 from the GOM, MAB, and SAB, respectively), based on a total of 159 individual annual production estimates for specific sites and years. Cloern et al. (2014) reported measurements as gross primary production, NPP, or unspecified; when given an option between these, we chose NPP first, unspecified second, and gross primary production last. Of the 24 estimates used here, 10 were of NPP, 2 were of gross primary production, and 12 were unspecified. For each subregion, we computed means and standard errors from these data.

Numerous methods estimate seagrass production in situ (Hemminga & Duarte, 2000), but spatial and temporal variability precludes their direct use for estimating areal NPP. Instead, we applied the approach of Hill et al. (2014), in which NPP is the product of standing carbon biomass (standing = aboveground + belowground) and an assumed specific growth rate (α). Following CEC (2016), we broke ENA into temperate and subtropical zones, which share a boundary in southern North Carolina. Mean area-specific aboveground dry biomass for the temperate zone (124 g m^{-2}) was obtained from 10 years of measurements for *Zostera marina* L. reported by Moore et al. (2000) for the Chesapeake Bay region. For the subtropical zone, we used the average (190 g m^{-2}) of three Gulf of Mexico sites: St. Joseph's Bay (Hill et al., 2014), St. George Sound, and Big Bend Seagrass Aquatic Preserve, with aboveground dry biomass values of 184, 166, and 218 g m^{-2}, respectively. Based on an analysis of allometric data presented by Duarte (1991), belowground dry biomass was estimated as 28 ± 9% of above ground biomass for the temperate (dominated by *Zostera marina* L.) and 208 ± 66% of aboveground dry biomass for the subtropical zone (dominated by *Thalassia testudinum* Banks ex König and *Syringodium filiforme* Kütz). The standing dry biomass was converted to standing carbon biomass by multiplying by 0.322 ± 0.018, a ratio we derived from an analysis of seagrass carbon content data of Duarte (1990). A specific growth rate of $\alpha = 7.3 \pm 1.8$ yr^{-1} (or 2 ± 0.5% d^{-1}) was adopted based on seasonal variability (Fourqurean et al., 2001; Lee & Dunton, 1997; Zimmerman et al., 1996, 1997, 2001, 2017). To compute spatially integrated fluxes, we used the seagrass areas in Table 1.

4.2.2. Estuarine Net Ecosystem Production (NEP_E)

Estuarine net ecosystem production (NEP_E) for U.S. East Coast estuaries was estimated by Herrmann et al. (2015), who employed an empirical model of NEP_E as a function of the molar ratio of dissolved inorganic nitrogen to TOC loadings from landward sources. We modified these estimates by (1) incorporating the new TOC fluxes from tidal wetlands reported here, which are based on improved area estimates, and (2) including the Canadian portion of the GOM. Using the Herrmann et al. (2015) model and their average estimate of the molar ratio of dissolved inorganic nitrogen to total nitrogen, 0.41, we calculated NEP_E on a unit

area basis for the St. John River estuary based on total nitrogen and TOC loading estimates from Clair et al. (2013) and the area of the St. John River estuary (Metcalfe et al., 1976). To estimate NEP_E of all Canadian GOM estuaries, we multiplied the St. John estimate by the freshwater scaling factor of 1.69 (section 3).

4.2.3. Riverine Input (R)

We used SPARROW (SPAtially Referenced Regression on Watersheds attributes) to provide estimates of riverine TOC fluxes to tidal estuarine waters. SPARROW is a spatially explicit statistical model that exploits data on land use, flow, and constituent concentration. The model was applied in the United States by Shih et al. (2010), based on a 1:500,000 scale RF1 (Reach File 1) classification of stream reaches and associated drainage areas (Nolan et al., 2002). Herrmann et al. (2015) modified SPARROW by distinguishing tidal wetlands as a separate wetland class and then using a literature-based estimate of the TOC yield from tidal wetlands. Here we made a further modification to SPARROW by using the updated (and more precise) National Wetland Inventory estimates of tidal wetland area as a replacement for the original National Land Cover Database estimates of wetland area in the coastal drainages of the SPARROW model. SPARROW coastal drainage areas are defined by the land area associated with "tidal" coastal reaches (RF1 coastal shoreline segments and associated drainage areas without RF1 stream reaches; termflag = 3 indicator, (Nolan et al., 2002)) and the terminal, most downstream "nontidal" RF1 stream reaches (termflag = 1 indicator) that are connected to estuaries. To ensure that the total areas of the RF1 reaches in coastal drainages remained the same, we assumed that the changes in wetland area, based on using the new wetland estimates, could be accounted for by making equivalent changes in the estimates of forested land area in the model. Accordingly, forested area was decreased (or increased) where the updated wetland area was greater than (or less than) the original wetland area. For the TOC fluxes to the GOM from Canada, we only had an estimate for the St. John River (Clair et al., 2013). To estimate the TOC fluxes from all rivers entering the GOM from Canada, we multiplied the St. John estimate by the freshwater scaling factor 1.69 (section 3). The standard error in riverine TOC input is automatically generated by SPARROW.

We used the Dynamic Land Ecosystem Model (DLEM) to provide estimates of riverine DIC fluxes to tidal estuarine waters. DLEM is a mechanistic terrestrial biogeochemical model that was recently used to simulate riverine DIC and TOC fluxes to coastal waters of ENA from 1901 to 2008 (Tian et al., 2015). DLEM simulations include the impacts of climate change and variability, land conversion, land management practices, atmospheric CO_2, and nitrogen deposition. We used DLEM estimates of the mean DIC flux from rivers for 1980–2008. Uncertainty estimates are lacking for DLEM, but this model appears to be as skillful as SPARROW (Tian et al., 2015), so, within each subregion, we assumed the fractional errors are the same as those of the riverine TOC input.

4.2.4. Exchange of CO_2 Between Estuaries and the Atmosphere (U_E)

A total of 16 literature estimates of U_E were compiled (Cai & Wang, 1998; Crosswell et al., 2014, 2012; Hunt et al., 2014, 2011; Jiang et al., 2008; Joesoef et al., 2015; Raymond & Hopkinson, 2003; Raymond et al., 2000; Wang & Cai, 2004; Table S2 in the supporting information), and means and standard errors were computed for each subregion.

4.2.5. Estuarine Burial (B_E)

Estimates of carbon burial in estuarine sediments of U.S. East Coast estuaries were taken from the model of Herrmann et al. (2015), which requires riverine total nitrogen loading and estuarine residence time as inputs. The model was applied to the St. John River estuary using the residence time of Metcalfe et al. (1976) and the riverine total nitrogen loading of Clair et al. (2013). To estimate burial in all Canadian GOM estuaries, we multiplied the St. John estimate by the freshwater scaling factor of 1.69 (section 3).

4.2.6. Estuarine Fluxes Computed as Residuals (L^O_{ES} and L^I_{ES})

As in Herrmann et al. (2015), L^O_{ES} was determined from the estuarine organic balance, equation (2b). Similarly, the estuarine inorganic carbon balance, equation (3b), was used to calculate L^I_{ES}.

4.3. Shelf Water Fluxes

4.3.1. Shelf Water Net Primary Production (NPP_S)

Syntheses of in situ shelf water net primary production measurements were derived from two major programs. The first is a set of National Marine Fisheries Service surveys from October 1977 to June 1982 in the MAB and GOM. More than 4,000 measurements were made with good spatial and seasonal coverage (O'Reilly & Busch, 1984; O'Reilly et al., 1987). From O'Reilly et al. (1987), we used the annual and spatial averages of primary production in four sectors of the MAB (MAS 1, 2, 3, and 4) and six sectors of the GOM (NT, GB 1, GB 2, GM 1, GM 2, and SS). Formal errors are not available for these averages; we subjectively

estimated that the standard error in each sector is a modest 30%, due the favorable spatial and temporal coverage of the measurements. As sector areas were unavailable, we digitized them from Figure 21.4 in O'Reilly et al. (1987). Subregional, area-weighted averages of NPP (g C m^{-2} yr^{-1}) were then computed. Subregional integrals (Tg C yr^{-1}) were computed using the actual areas of the MAB and GOM (Table 1). A similar analysis of this data set by Bisagni (2003) over a slightly different area produced essentially the same mean NPP per unit area as our analysis.

The second major source of in situ shelf water net primary production measurements is the Department of Energy's interdisciplinary study of the oceanography of the SAB. Menzel (1993) summarized the NPP measurements from this program, which were reported in greater detail in Yoder (1985) and Verity et al. (1993). Menzel (1993) provided mean NPP rates and areas of three sectors, which make up the bulk of the SAB as we have defined it. Again, no formal error estimate was provided, so we subjectively estimated the standard error in each sector to be 50%, which is higher than the estimated error in the MAB, due to the less favorable spatial and temporal coverage in the SAB. Subregional averages and integrals were computed as they were for the MAB and GOM. More recent estimates of SAB spatially integrated NPP by Jiang et al. (2010) are slightly higher than our estimates.

4.3.2. Shelf Water Net Ecosystem Production (NEP_S)

Estimates of shelf water net ecosystem production (NEP_S) were taken from the latest version (St-Laurent et al., 2017) of the process-based numerical model developed by the U.S. Eastern Continental Shelf (USECoS) project. The model has a typical horizontal resolution of 9 km, 30 vertical levels, and a domain that covers our study region. The model was integrated from November 2003 to December 2008 with realistic forcing at its boundaries with the atmosphere and open ocean. Building on previous versions (Cahill et al., 2016; Druon et al., 2010; Fennel et al., 2006; Hofmann et al., 2011), the biogeochemical module was adapted to include two phytoplankton and zooplankton size classes (Xiao & Friedrichs, 2014a, 2014b) and currently tracks 19 state variables, including DIC and several particulate and dissolved organic carbon pools that can be summed to TOC. We utilized NEP_S for each of the subregions and for each year from 2004 to 2008. Lacking a formal error estimate for NEP_S, we take 1 standard error to equal the standard deviation of annual NEP for each subregion. Though the model is mainly used for estimating NEP_S, we also compared its output with our estimates of several other terms in the shelf water carbon budget. Note that regridding of the subregion masks from Signorini et al. (2013) to the USECoS grid led to a modest 9% decline in ENA shelf water area.

4.3.3. Exchange of CO_2 Between Shelf Waters and the Atmosphere (U_S)

Signorini et al. (2013) made four distinct estimates of the exchange of CO_2 between ENA shelf waters and the atmosphere using two gas transfer velocity formulations and two estimates of surface ocean pCO_2 (one based solely on the data and the other from an algorithm that used remotely sensed sea surface temperature, remotely sensed chlorophyll, and a sea surface salinity climatology). The various approaches give broadly similar results and are generally in good agreement with previous studies. Here we adopt the results using the Ho et al. (2011) gas transfer velocity and the pCO_2 algorithm, which were applied over 2003–2010 in all three subregions of our study domain. Lacking a formal error estimate for the algorithm, we assumed that the standard error for each region is equal to the standard deviation of the annual flux. Note also that, whereas Signorini et al. (2013) treated Georges Bank and Nantucket Shoals as a separate region, we combined them with the GOM.

4.3.4. Burial in Shelf Sediments (B_S)

Shelf organic carbon burial fluxes were estimated by starting with a model of sedimentary organic carbon oxidation:

$$\log_{10}(C_{ox}) = a \log_{10}(z) + b \tag{6}$$

where C_{ox} is the oxidation rate in mmol m^{-2} d^{-1}, z is the water depth in meter, $a = -0.351 \pm 0.047$, and $b = 1.56 \pm 0.10$ (standard errors are given for a and b). Equation (6) is a least squares fit ($r^2 = 0.35$) to an updated global synthesis of Burdige (2007) based on 102 individual measurements, most of which (~80%) were made between depths of 1 and 500 m, appropriate for coastal waters. We estimated the mean C_{ox} in each region by using equation (5) with the mean depth (in our study domain) of the GOM, MAB, and SAB: 124, 44, and 30 m, respectively. Standard errors in C_{ox} were estimated as one half the maximum minus minimum C_{ox} given the standard error range in a and b. For muddy sediments, we assumed a burial

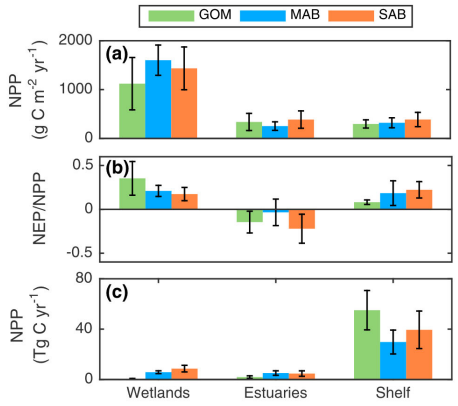

Figure 4. (a) Per-unit-area net primary production (NPP), (b) the ratio of net ecosystem production (NEP) to NPP, and (c) spatially integrated NPP for tidal wetlands, estuaries, and shelf waters in the three subregions (GOM = Gulf of Maine, MAB = Mid-Atlantic Bight, and SAB = South Atlantic Bight). Bars indicate ±2 standard errors.

efficiency (B_S divided by the POC flux to the sediments) of 0.25 (Burdige, 2007), in which case B_S/C_{ox} = 0.33 (assuming POC flux to sediments = B_S + C_{ox}). For sandy sediments, we assumed a burial efficiency, and hence B_S, equal to zero. We then assumed muddy sediment fractions of 30, 20, and 10% for the GOM, MAB, and SAB, respectively, based on a sediment distribution map in coastal waters of the eastern United States (Emery, 1968; Jahnke et al., 2008), and integrated over the shelf water areas in Table 1 to arrive at burial rates in units of Tg C yr^{-1}.

4.3.5. Shelf Fluxes Computed as Residuals (L^O_{SO}, L^I_{SO}, and L^T_{SO})

The net lateral transports of TOC, DIC, and total carbon from shelf waters to the open ocean (L^O_{SO}, L^I_{SO}, and L^T_{SO}, respectively) were computed as residuals using equations (2c), (3c), and (4c), respectively.

5. Results

All of the terms in the carbon budget equations (2)–(4) are presented for each subregion and for all the coastal waters of ENA on unit area and spatially integrated bases in the database provided as supporting information. In addition to the main budget terms, the database also contains a number of derived carbon flux variables discussed in the study but not explicitly included in the budget equations: NPP for tidal wetlands, estuarine plankton, estuarine seagrass, and shelf water plankton; HR; and tidal wetland degassing. In the supporting information and in the results that follow, the uncertainties are reported as ±2 standard errors, which approximate the 95% confidence range, except where noted. We first present NPP and the metabolic poise of each ecosystem and subregion and then present the organic, inorganic, and total carbon budgets for each ecosystem and subregion.

5.1. Net Primary Production and Metabolic Poise

NPP per unit area is much larger (by about a factor of 5) in tidal wetlands than in estuaries and shelf waters (Figure 4a). Thus, even though tidal wetland area is much smaller than estuarine area, spatially integrated NPP is higher for tidal wetlands (15.0 ± 2.9 Tg C yr^{-1}) than for estuaries (11.8 ± 3.0 Tg C yr^{-1}). Estuarine NPP is made up of planktonic NPP plus seagrass NPP. Seagrass NPP (per unit area of seagrass) of the SAB (1348 ± 444 g C m^{-2} yr^{-1}) is 3.6-fold higher than that of the MAB and GOM (374 ± 101 g C m^{-2} yr^{-1}), owing mainly to the larger contribution of belowground NPP in the SAB. ENA-averaged NPP of seagrass (801 ± 240 g C m^{-2} yr^{-1}) is larger than that of estuarine plankton (266 ± 77 g C m^{-2} yr^{-1}). However, because seagrass area is a small fraction of estuarine area (Table 1), only 13 ± 7% of ENA estuarine NPP is due to seagrass. Per-unit-area estuarine and shelf water NPP are remarkably similar to each other and relatively constant across the subregions (Figure 4a). Spatially integrated NPP for estuaries and shelves thus scales directly with area, with the GOM having the largest share of shelf water NPP and the MAB the largest share of estuarine NPP (Figure 4c).

The three ecosystems differ in their metabolic poise, as measured by NEP/NPP, with this ratio positive (net autotrophic) in tidal wetlands and shelf waters and negative (net heterotrophic) in estuaries (Figure 4b). Within each ecosystem, NEP/NPP is statistically similar across subregions, except for shelf waters, where the ratio is significantly higher in the SAB than in the GOM, owing to the fact that NEP of the SAB (86 ± 16 g C m^{-2} yr^{-1}) is about twice that of the GOM (24 ± 3 g C m^{-2} yr^{-1}). Average values of NEP/NPP across ENA in tidal wetlands, estuaries, and shelf waters are 0.20 ± 0.06, −0.13 ± 0.09, and 0.15 ± 0.04, respectively.

Although tidal wetlands have much greater fluxes per unit area, shelf waters, because of their large area, dominate the spatially integrated NPP of ENA coastal waters (Figure 4c); NPP for ENA is 151.0 ± 24.0 Tg C yr^{-1}, 82 ± 4% of which is in shelf waters. Similarly, spatially integrated ENA NEP (20.2 ± 4.4 Tg C yr^{-1}) is mainly due to shelf waters (18.8 ± 4.2 Tg C yr^{-1}), as the NEP rates in tidal wetlands (2.9 ± 0.8 Tg C yr^{-1}) and estuaries (−1.5 ± 1.0 Tg C yr^{-1}) are several times smaller in magnitude and partially offsetting. On the whole, ENA coastal waters are net autotrophic, with overall NEP/NPP equal to 0.13 ± 0.04.

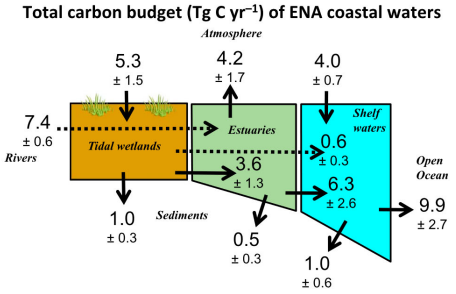

Figure 5. Total carbon budget (best estimate ±2 standard errors) for coastal waters of eastern North America (ENA). Dashed arrows represent carbon pathways not directly passing through either tidal wetlands or estuaries.

5.2. Total Carbon Budget

Figure 5 presents a summary budget for the study domain in terms of total carbon. Considering the *net* fluxes of total carbon at each of the four study domain boundaries (land, atmosphere, sediments, and open ocean) 59 ± 12% of the carbon entering the domain is from land (rivers) and the remaining 41 ± 12% (5.1 ± 2.3 Tg C yr^{-1}) is from the atmosphere, while 80 ± 9% of the domain's carbon loss is to the open ocean and the remaining 20 ± 9% (2.5 ± 0.7 Tg C yr^{-1}) is to the sediments (burial). Net lateral transfers between tidal wetlands and estuaries and between estuaries and shelf waters are comparable to carbon fluxes at the domain boundaries. For example, in terms of best estimates, the transfer of carbon from tidal wetlands to estuaries is larger than the amount of carbon buried in the study domain, and the transfer of carbon from estuaries to shelf waters is larger still and exceeds the net uptake of CO_2 from the atmosphere by the study domain. The transfer of carbon from tidal wetlands to shelf waters, on the other hand, is relatively small, owing to the fact that most tidal wetlands share their borders with estuaries.

Each ecosystem type contributes substantially to the overall carbon budget. Net uptake of CO_2 from the atmosphere is split nearly evenly between tidal wetlands and shelf waters, and CO_2 outgassing from estuaries offsets about half of this uptake. Similarly, each ecosystem contributes substantially to burial in the study domain, with 42 ± 12, 20 ± 9, and 38 ± 15% occurring in tidal wetlands, estuaries, and shelf waters, respectively. The importance of tidal wetlands and estuaries in the overall budget is remarkable given that they, respectively, make up only 2.4 and 8.9% of the study domain area.

5.3. Tidal Wetland Carbon Budgets

Of the four terms (NEP_W, B_W, U_W, and L_W) in the tidal wetland carbon budgets (Figures 6a, 6d, and 6g), net uptake from the atmosphere is the largest and burial is the smallest (note that L_{WE} and L_{WS} have been added together and represented as L_W in Figures 6a, 6d, and 6g). From the total carbon perspective (Figure 6h), 80 ± 7% of the net uptake from the atmosphere is balanced by net lateral export to estuaries and shelf waters, with only 20 ± 7% buried. Similarly, 64 ± 11% of organic carbon produced by NEP (Figure 6a) is exported laterally, with only 36 ± 11% buried. The inorganic carbon perspective reveals that CO_2 taken up from the atmosphere is split roughly evenly between losses to NEP (55 ± 15%) and net lateral export as DIC (45 ± 15%). Finally, the net lateral export is split nearly evenly between organic and inorganic forms, as dictated by the literature compilation (section 4.1.3). The SAB dominates most budget terms, which is not surprising because it contains most of the tidal wetland area (Table 1). Tidal wetland burial on a per unit area basis decreases toward the south, with rates in the GOM, MAB, and SAB equal to 211 ± 74, 152 ± 31, and 65 ± 30 g C m^{-2} yr^{-1}, respectively. This trend is mainly a result of the southward decline in carbon accumulation rate in the sediment cores used from the Ouyang and Lee (2014) compilation, with mean rates in the GOM, MAB, and SAB equal to 0.73 ± 0.34, 0.40 ± 0.08, and 0.23 ± 0.06 cm yr^{-1}. Corresponding mean carbon densities are relatively constant: 0.038 ± 0.005, 0.040 ± 0.005, and 0.027 ± 0.007 g C cm^{-3}. Most (52 ± 12%) of the tidal wetland burial occurs in the MAB because SAB burial rates per unit area are very low and GOM tidal wetland area is very low (Table 1).

Assuming that NPP_W is based mainly on CO_2 derived from the atmosphere, the degassing flux of CO_2 can be estimated as $NPP_W - U_W$, which turns out to equal 65 ± 12% of the atmospheric CO_2 taken up by tidal wetland plants as a result of NPP. Alternately, the degassing flux can be viewed in terms of respiration: nearly all of the CO_2 generated by heterotrophic respiration in tidal wetland soils (12.1 ± 3.5 Tg C yr^{-1}) is degassed (9.7 ± 3.7 Tg C yr^{-1}); the remaining 2.4 ± 1.2 Tg C yr^{-1} is exported laterally to nearby open waters.

5.4. Estuarine Carbon Budgets

Estuarine carbon budgets (Figures 6b, 6e, and 6h) are dominated by riverine input, net lateral exchanges with wetlands and shelf waters, and exchange with the atmosphere, with NEP and burial playing less important roles. This finding applies to ENA estuaries on average; individual estuaries or groups of estuaries will have

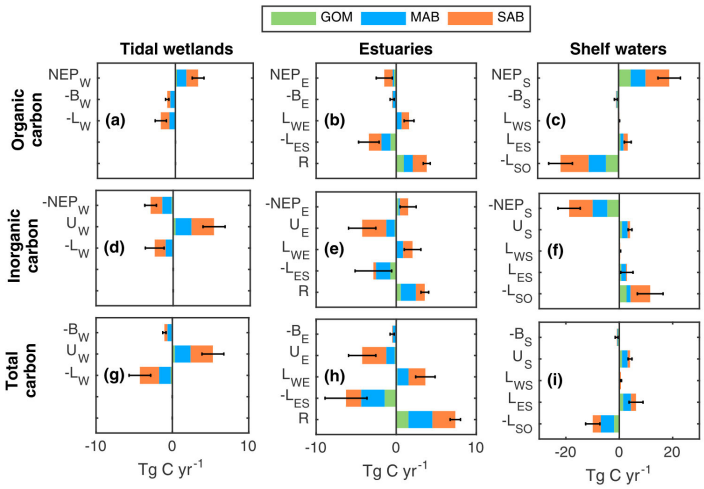

Figure 6. Budgets for (a–c) organic carbon, (d–f) inorganic carbon, and (g–i) total carbon in tidal wetlands, estuaries, and shelf waters. NEP = net ecosystem production, B = burial, U = uptake from atmosphere, R = riverine input, and L_{IJ} = net lateral transport from I to J, where W = wetlands, E = estuaries, and S = shelf waters. In the tidal wetland budgets, L_{WE} and L_{WS} have been added together and represented as L_W. GOM = Gulf of Maine, MAB = Mid-Atlantic Bight, and SAB = South Atlantic Bight. Bars indicate ±2 standard errors on the flux integrated across all subregions. Note the larger horizontal scale for shelf waters. To be consistent with equations (2)–(4), negative signs are placed on terms that appear on the right side of these equations (i.e., as sinks).

a different balance of terms. The carbon entering estuaries comes from rivers (67 ± 8%) and tidal wetlands (33 ± 8%), with losses dominated by net lateral export to shelf waters (57 ± 14%) and outgassing (39 ± 13%), leaving only a small loss (5 ± 3%) to burial (Figure 6h). The riverine carbon input is about evenly split between organic and inorganic forms. Despite similar streamflow among the three subregions (Table 1), the SAB and MAB, respectively, dominate the riverine input of organic and inorganic carbon, indicating relatively low carbon concentrations in GOM rivers. About one fifth of the total carbon input is from the GOM and the remainder is split about evenly between the MAB and SAB (Figure 6h).

Our estuarine NEP estimates and estuarine organic carbon budget (Figure 6b) are only slightly different from those of Herrmann et al. (2015), owing to the change in tidal wetland areas and the inclusion of the Canadian portion of the GOM. Figure 6e shows how NEP contributes to the overall inorganic carbon budget: net production of DIC in estuaries and upland DIC inputs support the net outgassing of CO_2 and net lateral export of DIC to shelf waters. The SAB dominates ENA net heterotrophy (Herrmann et al., 2015) and outgassing, the latter resulting from the much higher outgassing rates per unit area in SAB estuaries (246 ± 117 g C m^{-2} yr^{-1}) compared with estuaries in the MAB (52 ± 46 g C m^{-2} yr^{-1}), and GOM (35 ± 9 g C m^{-2} yr^{-1}). The MAB dominates the DIC net lateral export to shelf waters because the only other DIC loss term (outgassing) is relatively small in the MAB.

5.5. Shelf Water Carbon Budgets

NEP is a major term in organic and inorganic carbon budgets for shelf waters (Figures 6c and 6f), a striking contrast to those budgets for tidal wetlands and especially estuaries, on average (NEP may dominate in some estuaries). In the organic carbon budget, the production from NEP (84 ± 6% of the sources) is essentially balanced by export to the open ocean (96 ± 3% of the sinks); sources from estuaries and sinks from burial are relatively minor contributors, while wetland sources are insignificant. NEP is the sole sink of inorganic carbon in shelf waters, balanced by sources from the open ocean (62 ± 15%), the atmosphere (21 ± 6%),

Table 2
Estimates of the Uptake of Atmospheric CO_2 by Tidal Wetlands (U_W) in the Study Domain

Tidal wetland type	Location	Subregion	Year	Flux (g C m^{-2} yr^{-1})	Source
Salt marsh	Plum Island, MA	MAB	2012	256 ± 7	Forbrich and Giblin (2015)[a]
			2013	337 ± 6	
			2014	279 ± 7	
Salt marsh	Flax Pond, NY	MAB	1974	302	Houghton and Woodwell (1980)
Restored salt marsh	Hudson-Raritan Estuary, NJ	MAB	2009	−984	Schäfer et al. (2014)
			2011	65	
			2012	310	
Restored salt marsh	Hudson-Raritan Estuary, NJ	MAB	2011–2012	213	Artigas et al. (2015)
Tidal fresh marsh	Delaware Bay, NJ	MAB	2007	257	Weston et al. (2014)
			2008	−61	
Oligohaline marsh	Delaware Bay, NJ	MAB	2007	−94	Weston et al. (2014)
			2008	45	
Mesohaline marsh	Delaware Bay, NJ	MAB	2007	115	Weston et al. (2014)
			2008	171	
C3 brackish marsh	Chesapeake Bay, MD	MAB	1987–2005	1,300–2,500 (average 1,900)	Erickson et al. (2013)
C4 brackish marsh	Chesapeake Bay, MD	MAB	1987–2005	1100–2400 (average 1,500)	Erickson et al. (2013)
Salt marsh	Fowling Point, VA	MAB	2007	130	Kathilankal et al. (2008)
Tidal fresh marsh	Springfield Creek, SC	SAB	2009	295	Neubauer (2013)

Note. MAB = Mid-Atlantic Bight; SAB = South Atlantic Bight.
[a]Fluxes were measured from May 1 to October 31; we assumed fluxes outside of this period were zero.

estuaries (15 ± 13%), and wetlands (2 ± 1%). Terms in the total carbon budget (Figure 6i) tend to be smaller than terms in the organic and inorganic carbon budgets because NEP drops out and because the lateral exchanges with the open ocean go in different directions for organic and inorganic carbon. More TOC is lost to the open ocean than DIC is gained from the open ocean, resulting in a net loss of total carbon, which is largely balanced by net CO_2 uptake from the atmosphere and a lateral total carbon flux from estuaries.

The importance of individual subregions in shelf water carbon budgets depends on the process. Given the importance of NEP to shelf water budgets and the fact that the SAB dominates shelf water NEP (section 5.1), it is no surprise that the SAB is the most important subregion in shelf water organic and inorganic carbon budgets (Figures 6c and 6f). Even though the GOM is by far the largest shelf water subregion, its low NEP makes it only moderately important in the overall shelf water budgets. However, the GOM is the subregion that accounts for the greatest fraction (56 ± 28%) of shelf burial, which is due to its relatively large area and high fraction of muddy sediments; these effects outweigh its relatively low burial rate per unit area of muddy sediment, which is due to the GOM being the deepest shelf water subregion. Finally, the MAB is responsible for most (53 ± 9%) of shelf water uptake of atmospheric CO_2, owing to its relatively large fluxes per unit area (Signorini et al., 2013).

6. Discussion

6.1. Comparison With Previous Work in the Study Region

6.1.1. Uptake of Atmospheric CO_2 by Tidal Wetlands

Direct measurements of the gas flux between tidal wetlands and the atmosphere have been made at several locations along the U.S. East Coast (Table 2) and thus provide a comparison to our estimates of U_W, which are based on the application of equation (4a). Direct estimates of U_W in the study region are almost all positive, though they are all much lower than our mean estimate, except for the two Chesapeake Bay sites. At least three sites in Table 2 are not representative: the two restored sites and the oligohaline site in the Delaware Bay, which appears to be undergoing a transition to higher salinity. Taking the median value of U_W at the remaining eight sites (except for the Chesapeake Bay sites, where the mean was used) and then taking the median of those eight values yields a grand median of 287 g C m^{-2} yr^{-1}, slightly more than half of our estimated mean value of 524 ± 141 g C m^{-2} yr^{-1}.

There are many possible reasons for the discrepancy between direct measurements of U_W and our estimate here, including mismatches in time and space between the two types of estimates, overestimates of the

carbon loss terms from tidal wetlands (burial and tidal exchange), or underestimates of the CO_2 uptake by direct means. We suggest that uncertainty in our net lateral flux could be larger than we have estimated, mainly due to high spatial and temporal variability (e.g., seasonality and episodic events) that is not fully captured by the measurements, which are typically conducted over a few individual tidal cycles. High variability is also introduced by the opposite directions of the DOC and POC fluxes that make up the net lateral TOC flux. Although most studies show that tidal marshes are strong sources of DOC to adjacent waters, high variability has been reported in the rates and direction of POC exchange, with most studies indicating that coastal marshes act largely as sinks for chlorophyll and other particulate organic matter (Childers et al., 2000; C. D. Clark et al., 2014, 2008; Dankers et al., 1984; Eldridge & Cifuentes, 2000; Jordan et al., 1983; Moran et al., 1991; Nixon, 1980; Tobias & Neubauer, 2009; Tzortziou et al., 2011, 2008). In their review of salt marsh flux literature, Childers et al. (2000) reported that three of eight studies showed a net POC export from tidal wetlands of 11 to 128 g C m^{-2} yr^{-1}, while the remainder showed a net POC import of 3 to 140 g C m^{-2} yr^{-1}. Such a wide range of fluxes in both directions highlights the challenge of capturing the overall mean flux with a limited set of measurements. DIC net lateral flux measurements also have their challenges, as noted by Z. A. Wang et al. (2016), who used high-frequency data from in situ sensors to constrain the flux. The more traditional bottle sampling was found to lead to a significant underestimate of the flux, which may be why the Z. A. Wang et al. (2016) estimate is higher than others (Table S1). While this particular bias would increase the discrepancy between direct measurements of U_W and our calculation of U_W using mass balance, it highlights the difficulty of making accurate measurements of net lateral fluxes in tidal wetlands.

6.1.2. One-Dimensional Modeling of Eastern U.S. Estuaries

Our estuarine total carbon budget for ENA is similar to the carbon budget of 42 eastern U.S. estuaries based on 1-D mechanistic modeling (Laruelle et al., 2017) in that both studies find about 40% of upland inputs to be outgassed and 60% to be exported to shelf waters. Furthermore, the spatially integrated estuarine NEP of Laruelle et al. (2017) is the same as our central estimate, −1.4 Tg C yr^{-1}, which is also identical to that of Herrmann et al. (2015). However, our estimates of spatially integrated estuarine total carbon fluxes (Figure 5) are about a factor of 2 higher than those of Laruelle et al. (2017), who estimated riverine + tidal wetland inputs to be 4.6 Tg C yr^{-1}, outgassing to be 1.9 Tg C yr^{-1}, and export to shelf waters to be 2.7 Tg C yr^{-1}. Tidal wetland inputs were estimated by Laruelle et al. (2017) to be 0.6 Tg C yr^{-1}, or only one sixth of our estimate. Part of the difference in tidal wetland inputs is the lack of inclusion by Laruelle et al. (2017) of DIC, which we find to be as important as TOC. An additional reason for the difference may be the unit area yield of TOC from tidal wetlands because Laruelle et al. (2017), as we do, employ National Wetlands Inventory tidal wetland areas. For riverine inputs, Laruelle et al. (2017) used databases of riverine concentration and runoff for DIC and the global NEWS2 model for TOC. A detailed comparison between these sources and ours (DLEM and SPARROW) is needed to find out exactly where our riverine inputs differ with those of Laruelle et al. (2017). Whatever the cause of the difference, it probably propagates to the two main loss terms in the estuarine budget: outgassing and export to shelf waters. Laruelle et al. (2017) also ignore burial as a loss term, but this is a small fraction of total carbon losses in estuaries (Figure 5) and so is not a major concern.

Another important difference between the two studies is estuarine area, with ours (Table 1) almost a factor of 4 larger than the 10,815 km^2 of Laruelle et al. (2017), which is based on a segmentation of the coasts and related catchments known as COSCAT (Laruelle et al., 2013, 2015; Meybeck et al., 2006). In COSCAT, the eastern U.S. coast is represented as segment 837, which has an estuarine area of 15,000 km^2. In Laruelle et al. (2017) this segment was modified to include only "tidal" estuaries, which reduced the estuarine area to 10,850 km^2. We suggest that the coarse resolution of COSCAT results in a substantial underestimate of estuarine area. For example, a single ENA estuary, the Chesapeake Bay, has an area of 11,269 km^2 in our analysis, similar to the 11,666 km^2 reported by the Chesapeake Bay Program (2004), which is larger than the area of all U.S. East Coast estuaries in Laruelle et al. (2017).

6.1.3. The Chesapeake Bay

We also compare our estuarine organic carbon budget with data (Kemp et al., 1997) and a 3-D mechanistic model (Feng et al., 2015) of the Chesapeake Bay, a very large and well-studied ENA estuary that encompasses 29% of the estuarine area in the study domain. The mainstem of the bay (about half the area of the whole bay) is net autotrophic in the analysis of Kemp et al. (1997), with NEP equal to 0.28 ± 0.08 Tg C yr^{-1}. Feng et al. (2015) also find the mainstem bay to be net autotrophic, with NEP averaging 0.4 Tg C yr^{-1} and varying

dramatically from year to year ($<$ 0.1 to $>$0.6 Tg C yr^{-1}). Our budget employs the model of Herrmann et al. (2015), which estimates NEP for the whole bay (mainstem plus tributaries) to be −0.082 (−0.87, 0.28) Tg C yr^{-1} (best estimate and 95% confidence range). Our NEP estimate could be reconciled with that of Kemp et al. (1997) and Feng et al. (2015) if the tributaries of the Chesapeake Bay were net heterotrophic, which is feasible because the upper part of the mainstem Chesapeake Bay is net heterotrophic (Kemp et al., 1997) and many small or rapidly transiting estuaries are characterized by high net heterotrophy and high CO_2 degassing rates (Borges & Abril, 2011). Burial in the mainstem Chesapeake Bay was found by Kemp et al. (1997) to be 0.22 Tg C yr^{-1}, which compares well with the burial estimate of Feng et al. (2015), 0.3 Tg C yr^{-1}. Our estimate for the whole bay, based on the Herrmann et al. (2015), is 0.24 (0.077, 0.48) Tg C yr^{-1}. Thus, on a unit area basis, our burial estimate is about half that of Kemp et al. (1997) and Feng et al. (2015).

The mainstem Chesapeake Bay does not appear to be typical of ENA estuaries in terms of its organic carbon balance because it is net autotrophic, whereas ENA estuaries on the whole are net heterotrophic, though there are other exceptions, including Delaware Bay (Lebo & Sharp, 1992), another large MAB estuary. Furthermore, NEP plays a dominant role in the organic carbon budget of the mainstem Chesapeake Bay, approximately equal to the organic carbon inputs from external sources, mostly rivers and tributaries (Kemp et al., 1997). NEP plays a similarly important role in the nitrogen budget of the mainstem Bay (Feng et al., 2015). In contrast, for ENA as a whole, only 28 ± 19% of the organic carbon input from upland sources is consumed by NEP; most (63 ± 20%) of this input is exported to shelf waters. In summary, while it is tempting to use the large and well-studied mainstem Chesapeake Bay as representative of ENA estuaries, care should be taken in doing so.

6.1.4. ENA Shelf Water Studies

Spatially integrated NPP in the USECoS model is 30% lower than our estimate (Table 3), though the difference decreases to 23% if NPP per unit area is considered. Because the two estimates are from very different time periods, decadal variability at the subregional scale may explain the difference in the estimates. Balch et al. (2012) found a dramatic step decrease in GOM NPP in the mid-late 2000s. On the other hand, O'Brien (2015) found only a 2% increase in chlorophyll averaged over the northeast U.S. continental shelf and the Scotian shelf from 1998 to 2014. Another possible explanation for the model-data difference is a low-NPP bias in the model, consistent with the model's low-chlorophyll bias in most subregions and seasons, which is likely due to the coarse horizontal resolution of the model (St-Laurent et al., 2017). Differences are particularly large in the SAB and GOM, where the model NPP is lower than our estimate by 14 and 18 Tg C yr^{-1}, respectively (not shown). Had we used the NPP estimates of Bisagni (2003) and Jiang et al. (2010), the difference would be reduced by 4 Tg C yr^{-1} in the GOM and increased by 5 Tg C yr^{-1} in the SAB.

Uptake of CO_2 from the atmosphere simulated by the USECoS model is 90% greater than our satellite-based estimate (Signorini et al., 2013) (Table 3). Again, the main differences are in the SAB and GOM, where the model is in excess of our estimates by 1.2 and 2.4 Tg C yr^{-1}, respectively. The model may not be capturing the nutrient-rich Gulf Stream intrusions and associated upwelling that support much of the production (McClain et al., 1990; Yoder, 1985) and (speculatively) the outgassing associated with DIC-rich intrusions. The relatively high atmospheric CO_2 uptake by the GOM is consistent with a low-nitrate bias in the model during spring (St-Laurent et al., 2017), which suggests that the model also underestimates surface DIC and pCO_2, leading to excessive CO_2 uptake from the atmosphere.

Our estimates of net lateral exchange at the landward and seaward boundaries of shelf waters compare favorably with those of the USECoS model (Table 3). Despite the fact that the USECoS model does not consider tidal wetland inputs and poorly resolves estuaries (Feng et al., 2015), its estimates of net fluxes at the landward boundary of shelf waters are in good agreement with ours. This agreement stems first from both studies using similar riverine inputs, which dominate the carbon fluxes from land, and second that, in both studies, much of the riverine flux passes through estuaries without major modification, on average. Individual estuaries, such as the Chesapeake, may have NEP play a major role in carbon (Kemp et al., 1997) and nitrogen (Feng et al., 2015) transformations (section 6.1.3), but on average, most of the riverine carbon input to estuaries is exported to shelf waters. For example, 60% of upland inputs of organic carbon to U.S. East Coast estuaries is exported to shelf waters in the analysis of Herrmann et al. (2015). The agreement at the seaward boundary is a result of our use of USECoS NEP and the fact that the shelf

Table 3
Comparison of the USECoS Model Shelf Water Carbon Budget (Sum of GOM, MAB, and SAB) With This Study (Tg C yr^{-1})

Flux	USECoS model	This study
NPP_S	87 ± 9	124 ± 24
U_S	7.6 ± 1.6	4.0 ± 0.7
B_S	0.2 ± 0.0	1.0 ± 0.6
L^O_{SO}	21.8 ± 5.0	21.5 ± 11.6
L^I_{SO}	−9.3 ± 23.2	−11.6 ± 2.4
L^O_{ES}	3.3 ± 1.0	3.4 ± 1.3
L^I_{ES}	3.2 ± 3.8	2.9 ± 2.3
L^O_{WS}	–	0.3 ± 0.1
L^I_{WS}	–	0.3 ± 0.2
d(DIC)/d*t*	1.4 ± 24.2	–
d(TOC)/d*t*	−0.1 ± 1.2	–

Note. Uncertainty is reported as ±2 standard errors. For the USECoS model, we assume 1 standard error is equal to the standard deviation of the 5 annual averages during 2004–2008. NPPs = shelf water net primary production; MAB = Mid-Atlantic Bight; SAB = South Atlantic Bight; GOM = Gulf of Maine; USECoS = U.S. Eastern Continental Shelf; TOC = total organic carbon; DIC = dissolved inorganic carbon.

water organic and inorganic carbon budgets are dominated by a balance between NEP and net lateral exchange with the open ocean (section 5.5).

There are few additional estimates of the exchange of carbon between ENA shelf waters and the open ocean. DOC export from MAB shelf waters to the open ocean was estimated to be 6.2 Tg C yr^{-1} by Vlahos et al. (2002) using water mass analysis and 12.1 Tg C yr^{-1} by Mannino et al. (2016) using remote sensing and a hydrodynamic model. In our budget, we do not separate TOC into POC and DOC, but the USECoS model does. In that model, DOC export from the MAB to the open ocean is 4.1 ± 2.2 Tg C yr^{-1} or 63% of the corresponding TOC export from the MAB (64% for all of ENA). If we apply this fraction to our MAB TOC export, then we estimate MAB DOC export to be 4.1 ± 1.9 Tg C yr^{-1}, less than the estimates of Vlahos et al. (2002) and Mannino et al. (2016). An independent estimate of TOC export from the GOM to the open ocean of 1.3 ± 5.8 Tg C yr^{-1} was made by Charette et al. (2001), which agrees, within error, with our estimate of 4.7 ± 0.8 Tg C yr^{-1}. Our finding of an import of DIC to the MAB from the open ocean is also consistent with the finding of Z. A. Wang et al. (2013) that water leaving the MAB from the south is depleted in DIC with respect to water entering the MAB from the north.

We are aware of only two studies reporting direct burial measurements in ENA shelf sediments: Charette et al. (2001), who found a range of 3–10 g C m^{-2} yr^{-1} at four sites in the GOM, and Rowe et al. (1988), who found a rate of 4.3 g C m^{-2} yr^{-1} at one site in the northern MAB (estimates of burial on the MAB continental slope (Alperin et al., 2002) are probably not representative of the MAB shelf). These burial rates are somewhat higher than our GOM and MAB mean rates of 2.9 ± 2.8 and 2.8 ± 2.4 g C m^{-2} yr^{-1}, respectively. In both studies of direct measurements, burial was 2% of NPP, which can be compared to our lower ratios of 1% in the GOM, 0.9% in the MAB, and 0.4% in the SAB. The respective USECoS model ratios are lower still at 0.1, 0.6, and 0.3%, respectively. In summary, given the nearly 100% errors on our burial estimates, they are in agreement with other independent estimates.

It can be argued that the deficiencies in the USECoS model that lead to low NPP would also lead to low NEP. Hence, it may be preferable to use the NEP/NPP ratio from the USECoS model instead of its NEP. Had we done that, then shelf water NEP in our ENA budget would increase by 8.6 Tg C yr^{-1} to 27.4 ± 5.4 Tg C yr^{-1}; the import of DIC and the export of TOC to the open ocean, which are computed as residuals, would also increase by this amount, to 20.2 ± 6.0 and 30.1 ± 5.6 Tg C yr^{-1}. However, we chose to use the model's NEP directly because it must be consistent with model's nitrate and circulation fields, particularly at the model's open ocean boundary, fields that are produced reasonably well by the model, partly due to the realistic forcing at this boundary (St-Laurent et al., 2017).

6.2. Terms Not Considered in the Budget

6.2.1. Changing Carbon Inventory

The uptake of anthropogenic CO_2, which is causing a secular increase in the ocean's DIC inventory, is one violation of our steady state assumption. Specifically, no time-rate-of-change term is included in the inorganic and total carbon shelf budgets (equations (3c) and (4c)). To determine if this is a significant missing term in our shelf water carbon budgets, we first compute the time rate of change of the surface DIC concentration for a reference year of 2004 by assuming surface ocean pCO_2 = 370 μatm (Signorini et al., 2013) and surface ocean pCO_2 time-rate-of-change $dpCO_2/dt$ = 1.7 μatm yr^{-1} (Signorini et al., 2013); a buffer factor ($dpCO_2/pCO_2 \div d[DIC]dIC$) of 9.5 (Sabine et al., 2004); and a mean surface DIC concentration [DIC] = 2,050 mmol m^{-3} (Signorini et al., 2013). This yields a surface ocean d[DIC]/d*t* of 0.99 mmol m^{-3} yr^{-1}. Making the conservative assumption that the DIC concentration change is vertically uniform and estimating the volume to be 50 m times the shelf area (Table 1) yields a DIC inventory change of only 0.23 Tg C yr^{-1}, which is at least an order of magnitude smaller than other terms in the shelf water inorganic and total carbon budgets (Figures 6f and 6i), making the assumption of steady state in this case reasonable.

A related issue is the large interannual variability in the shelf water DIC inventory simulated by the USECoS model (Table 3). This variability, if real, should be taken into account for observational studies of the shelf water DIC budget that may be conducted over a short time period (less than a few years). This high variability also suggests that computing terms as residuals should only be done if the direct estimates of major fluxes in the inorganic carbon budget (uptake from the atmosphere and NEP) are long-term averages, which is what we have done by considering multiyear averages in these fluxes.

Given the global decline in tidal wetland coverage (Pendleton et al., 2012) as well as modifications of carbon cycle processes in tidal wetlands that are under hydrological management (Kroeger et al., 2017), another assumption that should be challenged is that of a constant standing stock of tidal wetland carbon, which allows us to drop time-rate-of-change terms in the tidal wetland organic carbon and total carbon budgets (equations (2a) and (4a)). Dahl and Stedman (2013) quantified changes in the area of U.S. coastal wetlands, which they defined as those wetlands in watersheds that drain directly to tidal water bodies; these wetlands are mostly nontidal. Despite the fact that coastal wetland area declined by 0.16% yr^{-1} from 2004 to 2009 in the eastern United States, saltwater wetland area did not change. Unfortunately, changes in the area of tidal freshwater wetlands were not reported. We estimate the tidal freshwater wetland carbon stock change for the eastern United States from the product of the fraction of tidal wetlands that are fresh (0.21, Hinson et al., 2017), the mass of carbon in the top 1 m of tidal wetland soil (650 Tg, Hinson et al., 2017), and the fractional loss rate of coastal wetland area (0.0016 per year, Dahl & Stedman, 2013). The resulting estimate, 0.22 Tg C yr^{-1}, is more than an order of magnitude smaller than the largest terms in the tidal wetland carbon budget (net lateral export and uptake from the atmosphere) and is about 20% of burial. While our assumption of steady state for tidal wetlands seems reasonable at this point, more work is needed to better quantify the role of tidal wetland loss in the carbon budget of coastal waters of the eastern United States.

6.2.2. Precipitation Effects

We have ignored effects of precipitation on the exchange of carbon between shelf waters and the atmosphere, effects which include the flux of carbon in precipitation, the enhancement of the gas transfer velocity due to rain, and enhancement of atmospheric CO_2 uptake by the ocean resulting from rain-induced depression of very near-surface pCO_2.

We make a rough estimate of the carbon flux in precipitation by assuming a precipitation rate of 1 m yr^{-1} (St-Laurent et al., 2017; Vlahos et al., 2002) and estimates of the concentration of DOC and DIC in rain. Willey et al. (2000) report DOC concentrations in rain of about 150 mmol m^{-3} over continents and 30–60 mmol m^{-3} over the open ocean. DIC concentration can be computed assuming equilibrium with atmospheric CO_2 and known values of CO_2 solubility and carbonic acid dissociation constants. For a temperature range of 5–20°C, we find DIC concentrations of 14–20 mmol m^{-3}, mostly as CO_2, consistent with several studies (e.g., Galloway et al., 1982; Willey et al., 2000). Adopting best estimates of DOC and DIC concentration of 70 and 17 mmol m^{-3}, respectively, the integrated organic, inorganic, and total carbon rainwater fluxes are 0.3, 0.1, and 0.4 Tg C yr^{-1}, respectively.

Ashton et al. (2016) found that the global ocean uptake of atmospheric CO_2 is increased by no more than 0.4% as a result of including rain enhancement of the transfer velocity using the parameterization of Harrison et al. (2012). Locally, effects generally did not exceed 0.1 g C m^{-2} yr^{-1}, which, if applied to ENA shelf waters, would increase the uptake by 1% or 0.04 Tg C yr^{-1}.

Finally, the addition of freshwater during precipitation events reduces surface ocean salinity, DIC, and alkalinity, which can reduce the surface carbon dioxide concentration (Dickson et al., 2007). Uptake would be enhanced over that estimated using typical surface pCO_2 measurements, which are made below the precipitation-influenced layer. Using data from biosphere experiments, Turk et al. (2010) modeled the impacts of this rain dilution effect and estimated an additional uptake of 0.72 g C m^{-2} yr^{-1} in the western equatorial Pacific Ocean, where the annual precipitation is about 3 m. Assuming that the effect scales with precipitation, we might expect an enhancement of atmospheric CO_2 uptake of 0.24 g C m^{-2} yr^{-1} or 0.09 Tg C yr^{-1} in ENA shelf waters.

Adding the three precipitation effects together, increases in the atmosphere-to-ocean fluxes of organic, inorganic, and total carbon are 0.3, 0.2, and 0.5 Tg C yr^{-1}, respectively. These would be minor terms in the shelf water carbon budgets, which are dominated by NEP and net lateral exchange with the open ocean (section 5.5).

The total precipitation enhancement is also about an order of magnitude smaller than our original estimate of atmospheric CO_2 uptake, though it is 50% of burial. In summary, a more rigorous approach to the estimate of carbon flux due to precipitation is unlikely to alter the ENA coastal water carbon budget in a major way.

6.2.3. Calcium Carbonate Fluxes

There has been very little research on calcium carbonate cycling in ENA coastal waters. Balch et al. (2008) found that only 1.4% of the carbon fixed in the GOM is calcium carbonate. However, based on the makeup of GOM sediments, Graziano et al. (2000) suggested that organic and inorganic carbon burial rates in this subregion may be similar. In SAB sediments, contributions from $CaCO_3$ are considerable, ranging from 4 to 22% (Marinelli et al., 1998), but rate processes have not been quantified. The considerable rates of calcium carbonate precipitation, dissolution, and burial in shallow tropical systems (Burdige et al., 2010; Burdige & Zimmerman, 2002; Burdige et al., 2008) suggest that calcium carbonate could contribute significantly to carbon budgets in the southern reaches of ENA coastal waters.

6.2.4. Photochemical Oxidation

DOC is photochemically oxidized to CO_2 and, to a lesser extent, carbon monoxide, a process we have ignored in our budgets but which has been argued to be important to the global marine carbon cycle (Miller & Zepp, 1995; W. Wang et al., 2009). Though CO_2 apparent quantum yields have been measured throughout ENA coastal waters (Del Vecchio et al., 2009; Johannessen & Miller, 2001; Reader & Miller, 2012; White et al., 2010; Ziolkowski & Miller, 2007), only two studies integrated their CO_2 production estimates over space, allowing comparison with our budgets. Del Vecchio et al. (2009) found MAB CO_2 photoproduction during May–August, the period of greatest photobleaching, to be 0.03–0.07 Tg C (0.02–0.05 Tg C when scaled to our MAB areal extent). Assuming that May–August accounts for half the annual production, then MAB CO_2 photoproduction is 0.04–0.08 Tg C yr^{-1}. Reader and Miller (2012) found that the inner SAB, which accounts for about one third of the SAB as we have defined it, produces CO_2 photochemically at the rate of about 0.15 Tg C yr^{-1}. Extrapolating to the whole SAB suggests a CO_2 production rate of about 0.4 Tg C yr^{-1}. This extrapolation is probably an overestimate because photo-oxidation rates will be lower in midshelf and outer-shelf waters, which have lower concentrations of colored dissolved organic matter and photochemically labile DOC. The estimated MAB and SAB CO_2 photoproduction rates are at least an order of magnitude smaller than the main budget terms in their respective subregions. Hence, the limited research available at this point suggests minor contributions of photochemical oxidation to ENA carbon budgets. In addition to direct photochemical oxidation, the photochemical formation of biologically labile compounds from DOC (Mopper et al., 2015) is likely an important mechanism of DOC remineralization that has yet to be quantified for ENA coastal waters.

6.2.5. Groundwater Inputs

Another poorly known carbon flux in the nearshore zone is that associated with groundwater. Discharge of fresh (terrestrial) groundwater occurs in estuaries and directly to the coastal ocean. Commonly, fresh groundwater mixes with saline groundwater and pore water in intertidal and subtidal soils and sediments, prior to discharge. As discussed by Kroeger and Charette (2008), mixing prior to discharge can complicate interpretation of constituent source in discharging fluids. In the current analysis, carbon of terrestrial provenance, carried by fresh groundwater, may represent additional carbon not accounted for in the riverine TOC and DIC flux estimates. Rates of fresh groundwater discharge show large spatial variability and are difficult to quantify, but global estimates suggest that the rate of discharge to estuaries and coasts (submarine groundwater discharge or SGD) is in the range of 6 to 10% of riverine discharge (Burnett et al., 2003). Concentrations of DIC and DOC in groundwater are also highly variable (e.g., Cai et al., 2003; Kroeger & Charette, 2008; Pabich et al., 2001; Santos et al., 2008; Sawyer et al., 2014; Szymczycha et al., 2017). Based on typical carbon concentrations and a global estimate of SGD rate, Cole et al. (2007) estimated that SGD of carbon is 27% of the riverine flux of carbon. Flux rates in specific regions may deviate substantially from that value, however. A new analysis along the Atlantic Coast of the United States estimates a rate of fresh groundwater discharge equivalent to 5.6% of riverine discharge (Befus et al., 2017), at the low end of the range of the ratio of global SGD to global riverine discharge, suggesting that the ENA ratio of SGD carbon flux to riverine carbon flux could be ~20% if the SGD carbon concentrations are typical. Groundwater thus has the potential to substantially alter our ENA coastal carbon budget.

6.2.6. Summary

The analysis above of changing carbon stocks, precipitation effects, calcium carbonate cycling, and photochemical oxidation suggests that ignoring these terms produces errors that are small (~0.1 to 1 Tg C yr^{-1})

compared to the largest terms (~10 Tg C yr^{-1}) in the ENA coastal carbon budget. On the other hand, groundwater fluxes could play a significant role. However, the uncertainties are considerable for all of the fluxes and cumulative effects of multiple missing terms may be significant.

6.3. Flux Variability

The major challenge in constructing regional coastal carbon budgets is spatial and temporal variability. We admit that the data syntheses, statistical models, and numerical models employed here only begin to capture this variability, and hence, our estimated errors may be too low. Most of our flux estimates incorporate seasonality (such as all of the NPP estimates) and many even incorporate interannual variability (such as riverine input of DIC, exchange of CO_2 between shelf waters and the atmosphere, and NEP of shelf waters). Some fluxes, such as burial, are measured or modeled in such a way that the estimates are essentially averages over many years. In reviewing all of the flux estimates in the budget, we find that one of them likely suffers from aliasing of the annual cycle: lateral exchange between tidal wetlands and estuaries. In addition to the challenges imposed by seasonal and interannual variability, extreme events are particularly vexing because they are difficult to sample and likely contribute substantially to coastal carbon fluxes. For example, Raymond and Saiers (2010) found that <5% of the hydrograph in U.S. forested rivers is responsible for 57% of the annual river DOC flux. The impact of tropical storms on coastal carbon cycling can be particularly dramatic, as has been shown for the exchange of atmospheric CO_2 with mangroves (Barr et al., 2012) and estuaries (Crosswell et al., 2014). The problem of sampling extreme events will only become more challenging as their frequency increases with global warming (Tebaldi et al., 2006).

6.4. How Representative Is Carbon Cycling in ENA Coastal Waters?

Global estimates of some coastal carbon fluxes—estuarine and shelf water NPP, estuarine and shelf air-water CO_2 exchange, tidal wetland and shelf burial, and net lateral exchange of DOC between shelf waters and the global ocean—afford us the opportunity to place our results in a broader context and assess how representative ENA coastal waters are of the global coastal ocean. First, however, we consider the proportion of the global coastal zone occupied by the three ecosystem types considered. Unfortunately, while the area of mangroves is well constrained at 0.14×10^6 km^2 (Giri et al., 2011), tidal marsh area ranges between 0.02 and 0.4×10^6 km^2 (Greenberg et al., 2006; Mcowen et al., 2017; Ouyang & Lee, 2014; Pendleton et al., 2012), leading to estimates of global tidal wetland area that vary from 0.16 to 0.54×10^6 km^2, more than a factor of 3. Global estuarine and shelf (shallower than 200 m) areas were estimated by Laruelle et al. (2013) to be 1.0×10^6 km^2 and 26×10^6 km^2, respectively. Thus, it appears that tidal wetlands, estuaries, and shelf waters encompass 0.6–2.0%, 3.6–3.7%, and 94.4–95.7%, respectively, of the global coastal zone, which can be compared with corresponding ENA fractions of 2.4, 8.9, and 88.7%. Hence, ENA appears to be more abundant in tidal wetlands and estuaries than the global average. However, tidal wetlands are very poorly mapped at the global scale and, if ENA estuaries are indicative (see section 6.1.2), then the Laruelle et al. (2013) global estuarine area may be too low. Hence, ENA coastal waters may be more representative in their makeup than suggested by the current global estimates of tidal wetland and estuarine area.

Primary production in ENA estuaries and shelf waters is very similar to corresponding global averages. Cloern et al. (2014) analyzed 1,148 estimates of annual primary production in 131 estuarine ecosystems and computed an overall mean of 252 g C m^{-2} yr^{-1} by first finding the median in each ecosystem and then taking the arithmetic mean of those medians. The ENA-wide average estuarine primary production we computed is 283 ± 78 g C m^{-2} yr^{-1}. The similarity to the global average may not be surprising because the data in the synthesis of Cloern et al. (2014) are heavily biased toward North America and Europe. Dunne et al. (2007) modeled the global distribution of primary production using satellite remote sensing. For regions shallower than 200 m, NPP was found to be 390 g C m^{-2} yr^{-1}, which is similar to our ENA shelf water average NPP of 326 ± 62 g C m^{-2} yr^{-1}. Hence, the similarity in NPP between estuaries and shelf waters in ENA (section 5.1) appears to be typical of the global coastal ocean.

As with NPP, air-water CO_2 exchange in ENA estuaries and shelf waters is very similar to corresponding global averages. Chen et al. (2013) analyzed air-water CO_2 flux estimates from 165 estuaries and computed a global area-weighted average outgassing of 93 g C m^{-2} yr^{-1}, which can be compared with the ENA average outgassing of 111 ± 45 g C m^{-2} yr^{-1}. The uptake of atmospheric CO_2 by continental shelf waters estimated by the data synthesis of Chen et al. (2013), the data synthesis of Laruelle et al. (2014), and the

biogeochemical model of Bourgeois et al. (2016) is 13, 8.6 ± 2.3 (95% confidence range), and 9.9 ± 4.6 (± 2 standard deviations of annual flux) g C m^{-2} yr^{-1}, respectively. These estimates bracket the ENA shelf water average uptake of 10.6 ± 1.9 g C m^{-2} yr^{-1}.

Our estimate of ENA B_W differs considerably from an estimate of the corresponding global average. From an analysis of data at 143 sites, Ouyang and Lee (2014) computed a global mean (± 2 standard errors) salt marsh burial rate of 245 ± 52 g C m^{-2} yr^{-1}, which is greater than our ENA mean rate of 103 ± 21 g C m^{-2} yr^{-1}. Part of this difference is due to the finding of Ouyang and Lee (2014) that carbon burial rate peaks at latitudes poleward of our study domain. This latitudinal dependency also accounts for some unknown fraction of the increase in burial rate we observe from the SAB to the GOM (section 5.3).

Similarly, our estimate of ENA burial in shelf sediments differs considerably from an estimate of the global average. Dunne et al. (2007) modeled the global distribution of burial using satellite-based NPP and empirical models. For regions shallower than 200 m, burial was found to be 40 g C m^{-2} yr^{-1}, which is much larger than our ENA shelf water burial average of 2.5 ± 1.5 g C m^{-2} yr^{-1}. This big difference in burial is largely due to the model of B_S/C_{ox}; the mean of B_S to the mean of C_{ox} is 0.03 in our approach (section 4.3.4), more than an order of magnitude smaller than the value of 0.8 estimated by Dunne et al. (2007). Our ratio of burial to NPP (1%) is also much smaller than the global value of 10% reported by Dunne et al. (2007).

Barrón and Duarte (2015) used a synthesis of 3,510 DOC concentration measurements and two estimates of water exchange between shelves and the open ocean to compute a global mean seaward DOC flux at the shelf break of 14.7 ± 6.6 and 90.0 ± 12.0 (± 2 standard errors) Gg C yr^{-1} per kilometer of shelf break. Assuming a total shelf break length of 2,000 km for ENA and the USECoS estimate of the dissolved fraction of the TOC export (64%), our DOC export per kilometer shelf break is 6.9 ± 0.7 Gg C yr^{-1}, which is below the lower limit of the considerably large range of values provided by Barrón and Duarte (2015).

In summary, ENA coastal waters appear to be globally representative when it comes to NPP and air-water CO_2 exchange in estuaries and shelf waters but to be on the low end of global averages of tidal wetland burial, shelf burial, and net lateral exchange of DOC between shelf waters and the open ocean. Differences in the former may reflect true spatial variability whereas those for the latter two may be methodological.

7. Conclusions

We have constructed a carbon budget for coastal waters of eastern North America, explicitly considering tidal wetlands, estuaries, and shelf waters, and separately accounting for organic carbon and inorganic carbon. To our knowledge, this is the first carbon budget constructed for a large coastline. Our main findings are the following.

1. NPP per unit area is much larger (by about a factor of 5) in tidal wetlands than in estuaries and shelf waters.
2. Tidal wetlands and shelf waters are net autotrophic, and estuaries are net heterotrophic; the study domain as a whole is net autotrophic.
3. Spatially integrated NPP and NEP are 151.0 ± 24.0 and 20.2 ± 4.4 Tg C yr^{-1}, respectively, and are dominated by shelf waters.
4. Considering the net fluxes of total carbon at the domain boundaries, 59 ± 12% of what enters is from rivers and 41 ± 12% is from the atmosphere, while 80 ± 9% of the carbon leaving is exported to the open ocean and 20 ± 9% is buried.
5. Net lateral transfers between tidal wetlands and estuaries and between estuaries and shelf waters are comparable to carbon fluxes at the domain boundaries.
6. Net uptake of CO_2 from the atmosphere is 5.1 ± 2.4 Tg C yr^{-1}; tidal wetlands and shelf waters take up about equal amounts of CO_2 and estuarine CO_2 outgassing offsets about half of this uptake.
7. Burial is 2.5 ± 0.7 Tg C yr^{-1}, with 42 ± 12, 20 ± 9, and 38 ± 15% occurring in tidal wetlands, estuaries, and shelf waters, respectively.
8. In tidal wetlands, 80 ± 7% of the net uptake from the atmosphere is balanced by net lateral export to estuaries and shelf waters, with only 20 ± 7% buried; 64 ± 11% of organic carbon produced by NEP is exported laterally, with only 36 ± 11% buried; and CO_2 taken up from the atmosphere is split roughly evenly between NEP (55 ± 15%) and net lateral export (45 ± 15%).

9. The carbon entering estuaries comes from rivers (67 ± 8%) and tidal wetlands (33 ± 8%), with losses dominated by net lateral export to shelf waters (57 ± 14%) and outgassing (39 ± 13%), leaving only a small loss (5 ± 3%) to burial.
10. In shelf waters, the production of organic carbon from NEP (84 ± 6% of the sources) is essentially balanced by export to the open ocean (96 ± 3% of the sinks); NEP is the sole sink of inorganic carbon in shelf waters, balanced by sources from the open ocean (62 ± 15%), the atmosphere (21 ± 6%), estuaries (15 ± 13%), and wetlands (2 ± 1%).

Comparison with prior work in the study area suggests further research is warranted. We find greater uptake of atmospheric CO_2 by tidal wetlands than the limited field studies available for comparison. Our estuarine budgets also differ substantially with numerical modeling and highlight the importance of accurate estimates of upland inputs and estuarine area. Our shelf water budgets highlight the need for independent NEP estimates as well as direct measurements of net lateral transport and burial. An assessment of missing terms in the budgets suggests, at this time, that the major terms have been captured. While research is needed to better quantify fluxes associated with precipitation, calcium carbonate, photochemistry, and changing carbon inventories, the most pressing need is to better quantify budget terms that are highly variable, poorly sampled, and potentially large. Fluxes computed as residuals also demand further study. Hence, priority should be given to all of the lateral exchanges, exchange of atmospheric CO_2 with tidal wetlands and estuaries, and shelf water NEP.

The likely path forward to wrestling with the large spatial and temporal variability of carbon cycle processes in the coastal zone is to employ empirical, process-based, and remote sensing models that are constrained by observations, as we have done here when possible. Recent progress in remote sensing models and process-based models, including those applied here, is encouraging. Corresponding models for tidal wetlands and their interaction with estuaries are only in their infancy (B. Clark et al., 2017). In many cases, direct and continuous measurements across spatial and temporal scales are extremely limited, which, in turn, hampers the development and application of data-constrained models. For example, for our study domain, we have only four direct measurements of the net lateral flux of DIC from wetlands, only two MAB estuaries with estimates of CO_2 outgassing, and only five sites where shelf burial has been measured. Other regions of the global coastal ocean may be in worse shape. For example, at the global scale, even the most basic information is lacking, such as accurate estimates of tidal wetland and estuarine area.

Acknowledgments
This research was supported by the NASA Interdisciplinary Science program (grant NNX14AF93G), the NASA Carbon Cycle Science Program (grant NNX14AM37G), the NASA Ocean Biology and Biogeochemistry Program (grant NNX11AD47G), and the National Science Foundation's Chemical Oceanography Program (grant OCE-1260574). Comments from an anonymous reviewer helped to improve this paper. This study was part of the North American Carbon Program. The data supporting the analysis and conclusions in this paper can be found in the supporting information. Any use of trade, firm, or product names is for descriptive purposes only and does not imply endorsement by the U.S. Government.

References

Alin, S., Siedlecki, S., Hales, B., Mathis, J., Evans, W., Stukel, M., et al. (2012). Coastal carbon synthesis for the continental shelf of the North American Pacific Coast (NAPC): Preliminary results. *Ocean Carbon and Biogeochemistry News*, *5*(1), 1–5.

Alongi, D. M. (2014). Carbon cycling and storage in mangrove forests. *Annual Review of Marine Science*, *6*(1), 195–219. https://doi.org/10.1146/annurev-marine-010213-135020

Alperin, M. J., Suayah, I. B., Benninger, L. K., & Martens, C. S. (2002). Modern organic carbon burial fluxes, recent sedimentation rates, and particle mixing rates from the upper continental slope near Cape Hatteras, North Carolina (USA). *Deep Sea Research Part II: Topical Studies in Oceanography*, *49*(20), 4645–4665. https://doi.org/10.1016/S0967-0645(02)00133-9

Artigas, F., Shin, J. Y., Hobble, C., Marti-Donati, A., Schäfer, K. V. R., & Pechmann, I. (2015). Long term carbon storage potential and CO_2 sink strength of a restored salt marsh in New Jersey. *Agricultural and Forest Meteorology*, *200*, 313–321. https://doi.org/10.1016/j.agrformet.2014.09.012

Ashton, I. G., Shutler, J. D., Land, P. E., Woolf, D. K., & Quartly, G. D. (2016). A sensitivity analysis of the impact of rain on regional and global sea-air fluxes of CO_2. *PLoS One*, *11*(9), e0161105. https://doi.org/10.1371/journal.pone.0161105

Balch, W. M., Drapeau, D. T., Bowler, B. C., Booth, E. S., Windecker, L. A., & Ashe, A. (2008). Space-time variability of carbon standing stocks and fixation rates in the Gulf of Maine, along the GNATS transect between Portland, ME, USA, and Yarmouth, Nova Scotia, Canada. *Journal of Plankton Research*, *30*(2), 119–139.

Balch, W. M., Drapeau, D., Bowler, B., & Huntington, T. G. (2012). Step-changes in the physical, chemical and biological characteristics of the Gulf of Maine, as documented by the GNATS time series. *Marine Ecology Progress Series*, *450*, 11–35. https://doi.org/10.3354/meps09555

Barr, J. G., Engel, V., Smith, T. J., & Fuentes, J. D. (2012). Hurricane disturbance and recovery of energy balance, CO_2 fluxes and canopy structure in a mangrove forest of the Florida Everglades. *Agricultural and Forest Meteorology*, *153*, 54–66. https://doi.org/10.1016/j.agrformet.2011.07.022

Barrón, C., & Duarte, C. M. (2015). Dissolved organic carbon pools and export from the coastal ocean. *Global Biogeochemical Cycles*, *29*, 1725–1738. https://doi.org/10.1002/2014GB005056

Bauer, J. E., Cai, W.-J., Raymond, P. A., Bianchi, T. S., Hopkinson, C. S., & Regnier, P. A. G. (2013). The changing carbon cycle of the coastal ocean. *Nature*, *504*(7478), 61–70. https://doi.org/10.1038/nature12857

Befus, K. M., Kroeger, K. D., Smith, C. G., & Swarzenski, P. W. (2017). The magnitude and origin of groundwater discharge to Eastern U.S. and Gulf of Mexico coastal waters. *Geophysical Research Letters*, *44*, 10,396–10,406. https://doi.org/10.1002/2017GL075238

Bisagni, J. J. (2003). Seasonal variability of nitrate supply and potential new production in the Gulf of Maine and Georges Bank regions. *Journal of Geophysical Research*, *108*(C11), 8015. https://doi.org/10.1029/2001JC001136

Borges, A. V., & Abril, G. (2011). Carbon dioxide and methane dynamics in estuaries. In E. Wolanski & D. S. McLusky (Eds.), *Treatise on Estuarine and Coastal Science* (Vol. 5, pp. 119–161). Waltham: Academic Press. https://doi.org/10.1016/B978-0-12-374711-2.00504-0

Borges, A. V., Delille, B., & Frankignoulle, M. (2005). Budgeting sinks and sources of CO_2 in the coastal ocean: Diversity of ecosystems counts. *Geophysical Research Letters*, *32*, L14601. https://doi.org/10.1029/2005GL023053

Bourgeois, T., Orr, J. C., Resplandy, L., Terhaar, J., Ethé, C., Gehlen, M., & Bopp, L. (2016). Coastal-ocean uptake of anthropogenic carbon. *Biogeosciences*, *13*(14), 4167–4185. https://doi.org/10.5194/bg-13-4167-2016

Bricker, S., Longstaff, B., Dennison, W., Jones, A., Boicourt, K., Wicks, C., & Woerner, J. (2007). *Effects of Nutrient Enrichment in the Nation's Estuaries: A Decade of Change*, *NOAA Coastal Ocean Program Decision Analysis Series* (Vol. 26, p. 328). Silver Spring, MD: National Centers for Coastal Ocean Science.

Burdige, D. J. (2007). Preservation of organic matter in marine sediments: Controls, mechanisms, and an imbalance in sediment organic carbon budgets? *Chemical Reviews*, *107*(2), 467–485. https://doi.org/10.1021/cr050347q

Burdige, D. J., Hu, X., & Zimmerman, R. C. (2010). The widespread occurrence of coupled carbonate dissolution/reprecipitation in surface sediments on the Bahamas Bank. *American Journal of Science*, *310*(6), 492–521. https://doi.org/10.2475/06.2010.03

Burdige, D. J., & Zimmerman, R. C. (2002). Impact of sea grass density on carbonate dissolution in Bahamian sediments. *Limnology and Oceanography*, *47*(6), 1751–1763. https://doi.org/10.4319/lo.2002.47.6.1751

Burdige, D. J., Zimmerman, R. C., & Hu, X. (2008). Rates of carbonate dissolution in permeable sediments estimated from pore-water profiles: The role of sea grasses. *Limnology and Oceanography*, *53*(2), 549–565. https://doi.org/10.4319/lo.2008.53.2.0549

Burnett, W. C., Bokuniewicz, H., Huettel, M., Moore, W. S., & Taniguchi, M. (2003). Groundwater and pore water inputs to the coastal zone. *Biogeochemistry*, *66*(1/2), 3–33. https://doi.org/10.1023/B:BIOG.0000006066.21240.53

Cahill, B., Wilkin, J., Fennel, K., Vandemark, D., & Friedrichs, M. A. M. (2016). Interannual and seasonal variability in air-sea CO_2 fluxes along the U.S. eastern continental shelf and their sensitivity to increasing air temperatures and variable winds. *Journal of Geophysical Research: Biogeosciences*, *121*, 295–311. https://doi.org/10.1002/2015JG002939

Cai, W.-J. (2011). Estuarine and coastal ocean carbon paradox: CO_2 sinks or sites of terrestrial carbon incineration? *Annual Review of Marine Science*, *3*(1), 123–145. https://doi.org/10.1146/annurev-marine-120709-142723

Cai, W.-J., Hu, X., Huang, W. J., Murrell, M. C., Lehrter, J. C., Lohrenz, S. E., et al. (2011). Acidification of subsurface coastal waters enhanced by eutrophication. *Nature Geoscience*, *4*(11), 766–770. https://doi.org/10.1038/ngeo1297

Cai, W.-J., & Wang, Y. (1998). The chemistry, fluxes, and sources of carbon dioxide in the estuarine waters of the Satilla and Altamaha Rivers, Georgia. *Limnology and Oceanography*, *43*(4), 657–668. https://doi.org/10.4319/lo.1998.43.4.0657

Cai, W.-J., Wang, Y., Krest, J., & Moore, W. (2003). The geochemistry of dissolved inorganic carbon in a surficial groundwater aquifer in North Inlet, South Carolina, and the carbon fluxes to the coastal ocean. *Geochimica et Cosmochimica Acta*, *67*(4), 631–639. https://doi.org/10.1016/S0016-7037(02)01167-5

CEC (2016). *North America's Blue Carbon: Assessing Seagrass, Salt Marsh and Mangrove Distribution and Carbon Sinks* (p. 54). Montreal, Canada: Commission for Environmental Cooperation.

Chapin, F. S., Woodwell, G. M., Randerson, J. T., Rastetter, E. B., Lovett, G. M., Baldocchi, D. D., et al. (2006). Reconciling carbon-cycle concepts, terminology, and methods. *Ecosystems*, *9*(7), 1041–1050. https://doi.org/10.1007/s10021-005-0105-7

Charette, M. A., Moran, S. B., Pike, S. M., & Smith, J. N. (2001). Investigating the carbon cycle in the Gulf of Maine using the natural tracer thorium 234. *Journal of Geophysical Research*, *106*(C6), 11,553–11,579. https://doi.org/10.1029/1999JC000277

Chavez, F. P., Takahashi, T., Cai, W.-J., Friederich, G., Hales, B., Wanninkhof, R., & Feely, R. A. (2007). Coastal oceans. In A. W. King, et al. (Eds.), *The First State of the Carbon Cycle Report (SOCCR): The North American Carbon Budget and Implications for the Global Carbon Cycle. A Report by the U.S. Climate Change Science Program and the Subcommittee on Global Change Research* (pp. 157–166). Asheville, NC, USA: National Oceanic and Atmospheric Administration, National Climatic Data Center.

Chen, C.-T., Huang, T.-H., Chen, Y.-C., Bai, Y., He, X., & Kang, Y. (2013). Air-sea exchanges of CO_2 in the world's coastal seas. *Biogeosciences*, *10*(10), 6509–6544. https://doi.org/10.5194/bg-10-6509-2013

Chesapeake Bay Program (2004). *Chesapeake Bay program analytical segmentation scheme: Revisions, decisions and rationales, 1983–2003* (p. 64). Maryland: Annapolis.

Childers, D. L., Day, J. W. Jr., & McKellar, N. Jr. (2000). Twenty more years of marsh and estuarine flux studies: Revisiting Nixon (1980). In M. Weinstein & D. A. Kreeger (Eds.), *Concepts and controversies in tidal marsh ecology* (pp. 391–423). Dordrecht: Kluwer Academic Publishing.

Chmura, G. L., Anisfeld, S. C., Cahoon, D. R., & Lynch, J. C. (2003). Global carbon sequestration in tidal, saline wetland soils. *Global Biogeochemical Cycles*, *17*(4), 1111. https://doi.org/10.1029/2002GB001917

Clair, T. A., Dennis, I. F., & Bélanger, S. (2013). Riverine nitrogen and carbon exports from the Canadian landmass to estuaries. *Biogeochemistry*, *115*(1-3), 195–211. https://doi.org/10.1007/s10533-013-9828-2

Clark, C. D., Aiona, P., Keller, J. K., & De Bruyn, W. J. (2014). Optical characterization and distribution of chromophoric dissolved organic matter (CDOM) in soil porewater from a salt marsh ecosystem. *Marine Ecology Progress Series*, *516*, 71–83. https://doi.org/10.3354/meps10833

Clark, C. D., Litz, L. P., & Grant, S. B. (2008). Saltmarshes as a source of chromophoric dissolved organic matter (CDOM) to Southern California coastal waters. *Limnology and Oceanography*, *53*(5), 1923–1933. https://doi.org/10.4319/lo.2008.53.5.1923

Clark, B., Long, W., Tzortziou, M., Neale, P., & Hood, R. (2017). Wind-driven dissolved organic matter dynamics in a Chesapeake Bay tidal marsh-estuary system. *Estuaries and Coasts*, 1–16. https://doi.org/10.1007/s12237-017-0295-1

Cloern, J. E., Foster, S. Q., & Kleckner, A. E. (2014). Phytoplankton primary production in the world's estuarine-coastal ecosystems. *Biogeosciences*, *11*(9), 2477–2501. https://doi.org/10.5194/bg-11-2477-2014

Coble, P. G., Robbins, L. L., Daly, K. L., Cai, W.-J., Fennel, K., & Lohrenz, S. E. (2010). A preliminary carbon budget for the Gulf of Mexico. *Ocean Carbon and Biogeochemistry News*, *3*(3), 1–4.

Cole, J. J., Prairie, Y. T., Caraco, N. F., McDowell, W. H., Tranvik, L. J., Striegl, R. G., et al. (2007). Plumbing the global carbon cycle: Integrating inland waters into the terrestrial carbon budget. *Ecosystems*, *10*(1), 172–185. https://doi.org/10.1007/s10021-006-9013-8

Continental Shelf Associates Inc. (1991). A comparison of marine productivity among outer continental shelf planning areas. Supplement—An evaluation of benthic habitat primary productivity. A final report for the U.S. Department of the Interior, Minerals Management Service, Herndon, VA. OCS study MMS 91-0001. Contract No. 14-35-0001-30487. 245 pp. + app.

Crosswell, J. R., Wetz, M. S., Hales, B., & Paerl, H. W. (2012). Air-water CO_2 fluxes in the microtidal Neuse River estuary, North Carolina. *Journal of Geophysical Research*, *117*, C08017. https://doi.org/10.1029/2012JC007925

Crosswell, J. R., Wetz, M. S., Hales, B., & Paerl, H. W. (2014). Extensive CO_2 emissions from shallow coastal waters during passage of Hurricane Irene (August 2011) over the mid-Atlantic Coast of the USA. *Limnology and Oceanography*, *59*(5), 1651–1665. https://doi.org/10.4319/lo.2014.59.5.1651

Dahl, T. E. (2011). *Status and trends of wetlands in the conterminous United States 2004 to 2009* (p. 108). Washington, DC: Fish and Wildlife Service, US Department of the Interior.

Dahl, T. E., & Stedman, S. M. (2013). *Status and trends of wetlands in the coastal watersheds of the conterminous United States 2004 to 2009* (p. 46). Washington, DC: U.S. Department of the Interior, Fish and Wildlife Service and National Oceanic and Atmospheric Administration, National Marine Fisheries Service.

Dankers, N., Binsbergen, M., Zegers, K., Laane, R., & van der Loeff, M. R. (1984). Transportation of water, particulate and dissolved organic and inorganic matter between a salt marsh and the Ems-Dollard estuary, The Netherlands, estuarine. *Coastal and Shelf Science*, *19*(2), 143–165. https://doi.org/10.1016/0272-7714(84)90061-1

Del Vecchio, R., Subramaniam, A., Schollaert Uz, S., Ballabrera-Poy, J., Brown, C. W., & Blough, N. V. (2009). Decadal time-series of SeaWiFS retrieved CDOM absorption and estimated CO_2 photoproduction on the continental shelf of the eastern United States. *Geophysical Research Letters*, *36*, L02602. https://doi.org/10.1029/2008GL036169

Diaz, R. J., & Rosenberg, R. (2008). Spreading dead zones and consequences for marine ecosystems. *Science*, *321*(5891), 926–929. https://doi.org/10.1126/science.1156401

Dickson, A. G., Sabine, C. L., & Christian, J. R. (Eds.) (2007). *Guide to best practices for ocean CO_2 measurements*, *PICES Special Publication* (Vol. 3, p. 191). Sidney, British Columbia, Canada: North Pacific Marine Science Organization.

Doney, S. C., Anderson, R., Bishop, J., Caldeira, K., Carlson, C., Carr, M.-E., et al. (2004). *Ocean Carbon and Climate Change (OCCC): An implementation strategy for U.S. ocean carbon cycle science* (p. 108). Boulder, CO: University Center for Atmospheric Research.

Druon, J. N., Mannino, A., Signorini, S., McClain, C., Friedrichs, M., Wilkin, J., & Fennel, K. (2010). Modeling the dynamics and export of dissolved organic matter in the northeastern U.S. continental shelf, estuarine. *Coastal and Shelf Science*, *88*(4), 488–507. https://doi.org/10.1016/j.ecss.2010.05.010

Duarte, C. (1990). Seagrass nutrient content. *Marine Ecology Progress Series*, *67*, 201–207. https://doi.org/10.3354/meps067201

Duarte, C. (1991). Allometric scaling of seagrass form and productivity. *Marine Ecology Progress Series*, *77*, 289–300. https://doi.org/10.3354/meps077289

Duarte, C., Middleburg, J., & Caraco, N. (2005). Major role of marine vegetation on the ocean carbon cycle. *Biogeosciences*, *2*(1), 1–8. https://doi.org/10.5194/bg-2-1-2005

Dunne, J. P., Sarmiento, J. L., & Gnanadesikan, A. (2007). A synthesis of global particle export from the surface ocean and cycling through the ocean interior and on the seafloor. *Global Biogeochemical Cycles*, *21*, GB4006. https://doi.org/10.1029/2006GB002907

Eldridge, P. M., & Cifuentes, L. A. (2000). A stable isotope model approach to estimating the contribution of organic matter from marshes to estuaries. In M. Weinstein & D. A. Kreeger (Eds.), *Concepts and controversies in tidal marsh ecology* (pp. 495–513). Dordrecht: Kluwer Academic Publishing.

Emery, K. O. (1968). Relict sediments on continental shelves of the world. *AAPG Bulletin*, *52*, 445–464.

Erickson, J. E., Peresta, G., Montovan, K. J., & Drake, B. G. (2013). Direct and indirect effects of elevated atmospheric CO_2 on net ecosystem production in a Chesapeake Bay tidal wetland. *Global Change Biology*, *19*, 3368–3378. https://doi.org/10.1111/gcb.12316

Feng, Y., Friedrichs, M. A. M., Wilkin, J., Tian, H., Yang, Q., Hofmann, E. E., et al. (2015). Chesapeake Bay nitrogen fluxes derived from a land-estuarine ocean biogeochemical modeling system: Model description, evaluation and nitrogen budgets. *Journal of Geophysical Research: Biogeosciences*, *120*, 1666–1695. https://doi.org/10.1002/2015JG002931

Fennel, K., Wilkin, J., Levin, J., Moisan, J., O'Reilly, J., & Haidvogel, D. (2006). Nitrogen cycling in the Middle Atlantic Bight: Results from a three-dimensional model and implications for the North Atlantic nitrogen budget. *Global Biogeochemical Cycles*, *20*, GB3007. https://doi.org/10.1029/2005GB002456

Forbrich, I., & Giblin, A. E. (2015). Marsh-atmosphere CO_2 exchange in a New England salt marsh. *Journal of Geophysical Research: Biogeosciences*, *120*, 1825–1838. https://doi.org/10.1002/2015JG003044

Fourqurean, J., Willsie, A., Rose, C., & Rutten, L. (2001). Spatial and temporal pattern in seagrass community composition and productivity in south Florida. *Marine Biology*, *138*(2), 341–354. https://doi.org/10.1007/s002270000448

Galloway, J. N., Likens, G. E., Keene, W. C., & Miller, J. M. (1982). The composition of precipitation in remote areas of the world. *Journal of Geophysical Research*, *87*(C11), 8771–8786. https://doi.org/10.1029/JC087iC11p08771

Giri, C., Ochieng, E., Tieszen, L. L., Zhu, Z., Singh, A., Loveland, T., et al. (2011). Status and distribution of mangrove forests of the world using Earth observation satellite data. *Global Ecology and Biogeography*, *20*(1), 154–159. https://doi.org/10.1111/j.1466-8238.2010.00584.x

Graziano, L. M., Balch, W. M., Drapeau, D., Bowler, B. C., Vaillancourt, R., & Dunford, S. (2000). Organic and inorganic carbon production in the Gulf of Maine. *Continental Shelf Research*, *20*(6), 685–705. https://doi.org/10.1016/S0278-4343(99)00091-6

Greenberg, R., Maldonado, J., Droege, S., & McDonald, M. V. (2006). Tidal marshes: A global perspective on the evolution and conservation of their terrestrial vertebrates. *Bioscience*, *56*(8), 675–685. https://doi.org/10.1641/0006-3568(2006)56%5B675:TMAGPO%5D2.0.CO;2

Gustavson, K. (2010). Coastal ecosystems and habitats. In J. Walmsley, et al. (Eds.), *State of the Gulf of Maine Report* (p. 20). Gulf of Maine Council on the Environment. Retrieved from http://www.gulfofmaine.org/2/wp-content/uploads/2014/03/coastal-ecosystems-and-habitats.pdf

Hales, B., Cai, W.-J., Mitchell, G., Sabine, C. L., & Schofield, O. (2008). North American continental margins: A synthesis and planning workshop. In *Report of the North American Continental Margins Working Group for the U.S. Carbon Cycle Scientific Steering Group and Interagency Working Group* (p. 110). Washington, DC: U. S. Carbon Cycle Science Program.

Hanson, A., & Calkins, L. (1996). *Wetlands of the Maritime Provinces: Revised documentation for the wetlands inventory* (Tech. Rep. 267, 67). Atlantic Region, Sackville, New Brunswick: Environment Canada, Canadian Wildlife Service.

Harrison, E. L., Veron, F., Ho, D. T., Reid, M. C., Orton, P., & McGillis, W. R. (2012). Nonlinear interaction between rain- and wind-induced air-water gas exchange. *Journal of Geophysical Research*, *117*, C03034. https://doi.org/10.1029/2011JC007693

Hemminga, M. A., & Duarte, C. M. (2000). *Seagrass Ecology*. Cambridge, UK: Cambridge University Press. https://doi.org/10.1017/CBO9780511525551

Herrmann, M., Najjar, R. G., Kemp, W. M., Alexander, R. B., Boyer, E. W., Cai, W.-J., et al. (2015). Net ecosystem production and organic carbon balance of U.S. East Coast estuaries: A synthesis approach. *Global Biogeochemical Cycles*, *29*, 96–111. https://doi.org/10.1002/2013GB004736

Hill, V. J., Zimmerman, R. C., Bissett, W. P., Dierssen, H., & Kohler, D. D. (2014). Evaluating light availability, seagrass biomass, and productivity using hyperspectral airborne remote sensing in Saint Joseph's Bay, Florida. *Estuaries and Coasts*, *37*(6), 1467–1489. https://doi.org/10.1007/s12237-013-9764-3

Hinson, A. L., Feagin, R. A., Eriksson, M., Najjar, R. G., Herrmann, M., Bianchi, T. S., et al. (2017). The spatial distribution of soil organic carbon in tidal wetland soils of the continental United States. *Global Change Biology*, *23*(12), 5468–5480. https://doi.org/10.1111/gcb.13811

Ho, D. T., Ferrón, S., Engel, V. C., Anderson, W. T., Swart, P. K., Price, R. M., & Barbero, L. (2017). Dissolved carbon biogeochemistry and export in mangrove-dominated rivers of the Florida Everglades. *Biogeosciences*, *14*(9), 2543–2559. https://doi.org/10.5194/bg-14-2543-2017

Ho, D. T., Wanninkhof, R., Schlosser, P., Ullman, D. S., Hebert, D., & Sullivan, K. F. (2011). Toward a universal relationship between wind speed and gas exchange: Gas transfer velocities measured with $^3He/SF_6$ during the Southern Ocean Gas Exchange Experiment. *Journal of Geophysical Research*, *116*, C00F04. https://doi.org/10.1029/2010JC006854

Hofmann, E. E., Cahill, B., Fennel, K., Friedrichs, M. A. M., Hyde, K., Lee, C., et al. (2011). Modeling the dynamics of continental shelf carbon. *Annual Review of Marine Science*, *3*(1), 93–122. https://doi.org/10.1146/annurev-marine-120709-142740

Hofmann, E., Druon, J. N., Fennel, K., Friedrichs, M., Haidvogel, D., Lee, C., et al. (2008). Eastern US continental shelf carbon budget: Integrating models, data assimilation, and analysis. *Oceanography*, *21*(1), 86–104. https://doi.org/10.5670/oceanog.2008.70

Hopkinson, C. S., & Smith, E. M. (2005). Estuarine respiration: An overview of benthic, pelagic, and whole system respiration. In P. A. del Giorgio & P. J. l. B. Williams (Eds.), *Respiration in aquatic ecosystems* (pp. 122–146). Oxford, UK: Oxford University Press. https://doi.org/10.1093/acprof:oso/9780198527084.003.0008

Houghton, R. A., & Woodwell, G. M. (1980). The flax pond ecosystem study: Exchanges of CO_2 between a salt marsh and the atmosphere. *Ecology*, *61*(6), 1434–1445. https://doi.org/10.2307/1939052

Hunt, C. W., Salisbury, J. E., & Vandemark, D. (2014). CO_2 input dynamics and air–sea exchange in a large New England estuary. *Estuaries and Coasts*, *37*(5), 1078–1091. https://doi.org/10.1007/s12237-013-9749-2

Hunt, C. W., Salisbury, J. E., Vandemark, D., & McGillis, W. (2011). Contrasting carbon dioxide inputs and exchange in three adjacent New England estuaries. *Estuaries and Coasts*, *34*(1), 68–77. https://doi.org/10.1007/s12237-010-9299-9

Jahnke, R., Cai, W. J., & Schofield, O. (2008). North America's Atlantic coast. In B. Hales, et al. (Eds.), *North American Continental Margins: A Synthesis and Planning Workshop. Report of the North American Continental Margins Working Group for the U.S. Carbon Cycle Scientific Steering Group and Interagency Working Group* (pp. 23–34). Washington, DC: U. S. Carbon Cycle Science Program.

Jiang, L.-Q., Cai, W.-J., & Wang, Y. (2008). A comparative study of carbon dioxide degassing in river- and marine-dominated estuaries. *Limnology and Oceanography*, *53*(6), 2603–2615. https://doi.org/10.4319/lo.2008.53.6.2603

Jiang, L.-Q., Cai, W.-J., Wang, Y., Diaz, J., Yager, P. L., & Hu, X. (2010). Pelagic community respiration on the continental shelf off Georgia, USA. *Biogeochemistry*, *98*(1-3), 101–113. https://doi.org/10.1007/s10533-009-9379-8

Joesoef, A., Huang, W.-J., Gao, Y., & Cai, W.-J. (2015). Air–water fluxes and sources of carbon dioxide in the Delaware estuary: Spatial and seasonal variability. *Biogeosciences*, *12*(20), 6085–6101. https://doi.org/10.5194/bg-12-6085-2015

Johannessen, S. C., & Miller, W. L. (2001). Quantum yield for the photochemical production of dissolved inorganic carbon in seawater. *Marine Chemistry*, *76*(4), 271–283. https://doi.org/10.1016/S0304-4203(01)00067-6

Jordan, T. E., Correll, D. L., & Whigham, D. F. (1983). Nutrient flux in the Rhode River: Tidal exchange of nutrients by brackish marshes, estuarine. *Coastal and Shelf Science*, *17*(6), 651–667. https://doi.org/10.1016/0272-7714(83)90032-X

Kathilankal, J. C., Mozdzer, T. J., Fuentes, J. D., D'Odorico, P., McGlathery, K. J., & Zieman, J. C. (2008). Tidal influences on carbon assimilation by a salt marsh. *Environmental Research Letters*, *3*(4), 044010. https://doi.org/10.1088/1748-9326/3/4/044010

Kemp, W. M., Smith, E. M., Marvin-DiPasquale, M., & Boynton, W. R. (1997). Organic carbon balance and net ecosystem metabolism in Chesapeake Bay. *Marine Ecology Progress Series*, *150*, 229–248. https://doi.org/10.3354/meps150229

Krause-Jensen, D., & Duarte, C. M. (2016). Substantial role of macroalgae in marine carbon sequestration. *Nature Geoscience*, *9*(10), 737–742. https://doi.org/10.1038/ngeo2790

Kroeger, K. D., & Charette, M. A. (2008). Nitrogen biogeochemistry of submarine groundwater discharge. *Limnology and Oceanography*, *53*(3), 1025–1039. https://doi.org/10.4319/lo.2008.53.3.1025

Kroeger, K. D., Crooks, S., Moseman-Valtierra, S., & Tang, J. (2017). Restoring tides to reduce methane emissions in impounded wetlands: A new and potent blue carbon climate change intervention. *Scientific Reports*, *7*(1), 11914. https://doi.org/10.1038/s41598-017-12138-4

Laruelle, G. G., Dürr, H. H., Lauerwald, R., Hartmann, J., Slomp, C. P., Goossens, N., & Regnier, P. A. G. (2013). Global multi-scale segmentation of continental and coastal waters from the watersheds to the continental margins. *Hydrology and Earth System Sciences*, *17*(5), 2029–2051. https://doi.org/10.5194/hess-17-2029-2013

Laruelle, G. G., Goossens, N., Arndt, S., Cai, W. J., & Regnier, P. (2017). Air–water CO_2 evasion from US East Coast estuaries. *Biogeosciences*, *14*(9), 2441–2468. https://doi.org/10.5194/bg-14-2441-2017

Laruelle, G. G., Lauerwald, R., Pfeil, B., & Regnier, P. (2014). Regionalized global budget of the CO_2 exchange at the air-water interface in continental shelf seas. *Global Biogeochemical Cycles*, *28*, 1199–1214. https://doi.org/10.1002/2014GB004832

Laruelle, G. G., Lauerwald, R., Rotschi, J., Raymond, P. A., Hartmann, J., & Regnier, P. (2015). Seasonal response of air-water CO_2 exchange along the land-ocean aquatic continuum of the northeast North American coast. *Biogeosciences*, *12*(5), 1447–1458. https://doi.org/10.5194/bg-12-1447-2015

Lebo, M. E., & Sharp, J. H. (1992). Modeling phosphorus cycling in a well-mixed coastal plain estuary, estuarine. *Coastal and Shelf Science*, *35*(3), 235–252. https://doi.org/10.1016/S0272-7714(05)80046-0

Lee, K., & Dunton, K. (1997). Effect of in situ light reduction on the maintenance, growth and partitioning of carbon resources in Thalassia Testudinum banks ex König. *Journal of Experimental Marine Biology and Ecology*, *210*(1), 53–73. https://doi.org/10.1016/S0022-0981(96)02720-7

MacIntyre, H. L., Geider, R. J., & Miller, D. C. (1996). Microphytobenthos: The ecological role of the "secret garden" of unvegetated, shallow-water marine habitats. I. Distribution, abundance and primary production. *Estuaries*, *19*(2), 186–201.

Mannino, A., Signorini, S. R., Novak, M. G., Wilkin, J., Friedrichs, M. A. M., & Najjar, R. G. (2016). Dissolved organic carbon fluxes in the Middle Atlantic Bight: An integrated approach based on satellite data and ocean model products. *Journal of Geophysical Research: Biogeosciences*, *121*, 312–336. https://doi.org/10.1002/2015JG00303

Marinelli, R. L., Jahnke, R. A., Craven, D. B., Nelson, J. R., & Eckman, J. E. (1998). Sediment nutrient dynamics on the South Atlantic Bight continental shelf. *Limnology and Oceanography*, *43*(6), 1305–1320. https://doi.org/10.4319/lo.1998.43.6.1305

Mathis, J. T., & Bates, N. R. (2010). The marine carbon cycle of the Arctic Ocean: Some thoughts about the controls on air-sea CO_2 exchanges and responses to ocean acidification. *Ocean Carbon and Biogeochemistry News*, *3*(2), 1–5.

McAdie, H. G. (1995). *Atmospheric deposition to the Gulf of Maine* (p. 73). Ottawa, Ontario and Washington, DC: International Joint Commission.

McClain, C., Ishizaka, J., & Hofmann, E. (1990). Estimation of phytoplankton pigment changes on the southeastern US continental shelf from a sequence of CZCS images and a coupled physical-biological model. *Journal of Geophysical Research*, *95*(C11), 20,213–20,235. https://doi.org/10.1029/JC095iC11p20213

McKinley, G., Urban, N., Bennington, V., Pilcher, D., & McDonald, C. (2011). Preliminary carbon budgets for the Laurentian Great Lakes. *Ocean Carbon and Biogeochemistry News*, *4*(2), 1–7.

Mcowen, C., Weatherdon, L., Bochove, J. W., Sullivan, E., Blyth, S., Zockler, C., et al. (2017). A global map of saltmarshes. *Biodiversity Data Journal*, *5*, e11764. https://doi.org/10.3897/BDJ.5.e11764

Mendelssohn, I. A., & Morris, J. T. (2000). Eco-physiological controls on the productivity of Spartina Alterniflora Loisel. In M. P. Weinstein & D. A. Kreeger (Eds.), *Concepts and Controversies in Tidal Marsh Ecology* (pp. 59–80). Netherlands: Springer.

Menzel, D. W. (1993). *Ocean processes: US Southeast continental shelf. A summary of research conducted in the South Atlantic Bight under the auspices of the US Department of Energy From 1977 to 1991* (p. 112). Savannah: US Dept. of Energy, Office of Scientific and Technical Information.

Metcalfe, C. D., Dadswell, M. J., Gillis, G. F., & Thomas, M. L. H. (1976). *Physical, chemical, and biological parameters of the Saint John River Estuary* (Tech. Rep. 686, 41 pp.), New Brunswick, Canada: Fisheries and Marine Service, Environment Canada.

Meybeck, M., Dürr, H. H., & Vörösmarty, C. J. (2006). Global coastal segmentation and its river catchment contributors: A new look at land-ocean linkage. *Global Biogeochemical Cycles*, *20*, GB1S90. https://doi.org/10.1029/2005GB002540

Miller, W. L., & Zepp, R. G. (1995). Photochemical production of dissolved inorganic carbon from terrestrial organic matter: Significance to the oceanic organic carbon cycle. *Geophysical Research Letters*, *22*(4), 417–420. https://doi.org/10.1029/94GL03344

Moore, K. A., Wilcox, D. J., & Orth, R. J. (2000). Analysis of the abundance of submersed aquatic vegetation communities in the Chesapeake Bay. *Estuaries*, *23*(1), 115–127. https://doi.org/10.2307/1353229

Mopper, K., Kieber, D. J., & Stubbins, A. (2015). Chapter 8, Marine photochemistry of organic matter: Processes and impacts. In D. A. Hansell & C. A. Carlson (Eds.), *Biogeochemistry of marine dissolved organic matter* (2nd ed., pp. 389–450). Amsterdam, Netherlands: Academic Press. https://doi.org/10.1016/B978-0-12-405940-5.00008-X

Moran, M. A., Wicks, R. J., & Hodson, R. E. (1991). Export of dissolved organic matter from a mangrove swamp ecosystem: Evidence from natural fluorescence, dissolved lignin phenols, and bacterial secondary production. *Marine Ecology Progress Series*, *76*(2), 175–184. https://doi.org/10.3354/meps076175

Morris, J. T., & Whiting, G. J. (1986). Emission of gaseous carbon dioxide from salt-marsh sediments and its relation to other carbon losses. *Estuaries and Coasts*, *9*(1), 9–19. https://doi.org/10.2307/1352188

Najjar, R. G., Friedrichs, M. A. M., & Cai, W.-J. (Eds.) (2012). *Report of the U.S. East Coast Carbon Cycle Synthesis Workshop* (p. 34). Greenbelt, MD: Ocean Carbon and Biogeochemistry Program and North American Carbon Program.

Neubauer, S. C. (2013). Ecosystem responses of a tidal freshwater marsh experiencing saltwater intrusion and altered hydrology. *Estuaries and Coasts*, *36*(3), 491–507. https://doi.org/10.1007/s12237-011-9455-x

Neubauer, S. C., & Anderson, I. C. (2003). Transport of dissolved inorganic carbon from a tidal freshwater marsh to the York River estuary. *Limnology and Oceanography*, *48*(1), 299–307. https://doi.org/10.4319/lo.2003.48.1.0299

Nixon, S. W. (1980). Between coastal marshes and coastal waters: A review of twenty years of speculation and research on the role of salt marshes in estuarine productivity and water chemistry. In P. Hamilton & K. B. MacDonald (Eds.), *Estuarine and wetland processes* (pp. 437–525). New York: Plenum Press. https://doi.org/10.1007/978-1-4757-5177-2_20

NOAA (1975). The coastline of the United States, NOAA/PA 71046.

NOAA (1985). *National estuarine inventory data atlas. Volume 1: Physical and hydrologic characteristics.* Washington, DC: National Ocean Service, National Oceanic and Atmospheric Administration.

Nolan, J. V., Brakebill, J. W., Alexander, R. B., & Schwarz, G. E. (2002). Enhanced river reach file 2, U.S. Geol. Surv. Open File Rep. 02-40, Reston, VA.

O'Brien, T. D. (2015). Indicator: Ocean chlorophyll concentrations. Retrieved from https://data.globalchange.gov/report/indicator-ocean-chlorophyll-concentrations, Accessed August 7, 2017

O'Reilly, J., & Busch, D. A. (1984). Phytoplankton primary production on the northwestern Atlantic shelf, rapports et Proces-verbaux des Réunions. *Conseil International pour l'Éxploration de la Mer*, *183*, 255–268.

O'Reilly, J., Evans-Zetlin, C., & Busch, D. A. (1987). Primary production. In R. H. Backus (Ed.), *Georges bank* (pp. 220–233). Cambridge, MA: MIT Press.

Ouyang, X., & Lee, S. (2014). Updated estimates of carbon accumulation rates in coastal marsh sediments. *Biogeosciences*, *11*(18), 5057–5071. https://doi.org/10.5194/bg-11-5057-2014

Pabich, W. J., Valiela, I., & Hemond, H. F. (2001). Relationship between DOC concentration and vadose zone thickness and depth below water table in groundwater of Cape Cod, USA. *Biogeochemistry*, *55*(3), 247–268. https://doi.org/10.1023/A:1011842918260

Pendleton, L., Donato, D. C., Murray, B. C., Crooks, S., Jenkins, W. A., Sifleet, S., et al. (2012). Estimating global "blue carbon" emissions from conversion and degradation of vegetated coastal ecosystems. *PLoS One*, *7*(9), e43542. https://doi.org/10.1371/journal.pone.0043542

Raymond, P. A., Bauer, J. E., & Cole, J. J. (2000). Atmospheric CO_2 evasion, dissolved inorganic carbon production, and net heterotrophy in the York River estuary. *Limnology and Oceanography*, *45*(8), 1707–1717. https://doi.org/10.4319/lo.2000.45.8.1707

Raymond, P. A., & Hopkinson, C. S. (2003). Ecosystem modulation of dissolved carbon age in a temperate marsh-dominated estuary. *Ecosystems*, *6*(7), 694–705. https://doi.org/10.1007/s10021-002-0213-6

Raymond, P. A., & Saiers, J. E. (2010). Event controlled DOC export from forested watersheds. *Biogeochemistry*, *100*(1-3), 197–209. https://doi.org/10.1007/s10533-010-9416-7

Reader, H., & Miller, W. (2012). Variability of carbon monoxide and carbon dioxide apparent quantum yield spectra in three coastal estuaries of the South Atlantic Bight. *Biogeosciences*, *9*(11), 4279–4294. https://doi.org/10.5194/bg-9-4279-2012

Regnier, P., Friedlingstein, P., Ciais, P., Mackenzie, F. T., Gruber, N., Janssens, I. A., et al. (2013). Anthropogenic perturbation of the carbon fluxes from land to ocean. *Nature Geoscience*, *6*(8), 597–607. https://doi.org/10.1038/ngeo1830

Rowe, G. T., Theroux, R., Phoel, W., Quinby, H., Wilke, R., Koschoreck, D., et al. (1988). Benthic carbon budgets for the continental shelf south of New England. *Continental Shelf Research*, *8*(5-7), 511–527. https://doi.org/10.1016/0278-4343(88)90066-0

Sabine, C. L., Feely, R. A., Gruber, N., Key, R. M., Lee, K., Bullister, J. L., et al. (2004). The oceanic sink for anthropogenic CO_2. *Science*, *305*(5682), 367–371. https://doi.org/10.1126/science.1097403

Santos, I. R. S., Burnett, W. C., Chanton, J., Mwashote, B., Suryaputra, I. G., & Dittmar, T. (2008). Nutrient biogeochemistry in a Gulf of Mexico subterranean estuary and groundwater-derived fluxes to the coastal ocean. *Limnology and Oceanography*, *53*(2), 705–718. https://doi.org/10.4319/lo.2008.53.2.0705

Sawyer, A. H., Lazareva, O., Kroeger, K. D., Crespo, K., Chan, C. S., Stieglitz, T., & Michael, H. A. (2014). Stratigraphic controls on fluid and solute fluxes across the sediment—Water interface of an estuary. *Limnology and Oceanography*, *59*(3), 997–1010. https://doi.org/10.4319/lo.2014.59.3.0997

Schäfer, K. V. R., Tripathee, R., Artigas, F., Morin, T. H., & Bohrer, G. (2014). Carbon dioxide fluxes of an urban tidal marsh in the Hudson-Raritan estuary. *Journal of Geophysical Research: Biogeosciences*, *119*, 2065–2081. https://doi.org/10.1002/2014JG002703

Shih, J.-S., Alexander, R. B., Smith, R. A., Boyer, E. W., Schwarz, G. E., & Chung, S. (2010). An initial SPARROW model of land use and in-stream controls on total organic carbon in streams of the conterminous United States, U.S. Geol. Surv. Open File Rep. 2010–1276, 22 pp., Reston, VA.

Signorini, S., Mannino, A., Friedrichs, M. A. M., Najjar, R. G., Cai, W.-J., Salisbury, J. E., et al. (2013). Surface ocean pCO_2 seasonality and sea-air CO_2 flux estimates for the North American east coast. *Journal of Geophysical Research: Oceans*, *118*, 5439–5460. https://doi.org/10.1002/jgrc.20369

Squires, G. L. (2001). *Practical Physics* (p. 212). Cambridge, UK: Cambridge University Press. https://doi.org/10.1017/CBO9781139164498

Stets, E. G., & Striegl, R. G. (2012). Carbon export by rivers draining the conterminous United States. *Inland Waters*, *2*(4), 177–184. https://doi.org/10.5268/IW-2.4.510

St-Laurent, P., Friedrichs, M. A. M., Najjar, R. G., Herrmann, M., Miller, S., Martins, D., & Wilkin, J. (2017). Impacts of atmospheric nitrogen deposition on surface waters of the western North Atlantic mitigated by multiple feedbacks. *Journal of Geophysical Research: Oceans*, *122*, 8406–8426. https://doi.org/10.1002/2017JC013072

Szymczycha, B., Kroeger, K. D., Crusius, J., & Bratton, J. F. (2017). Depth of vadose zone controls aquifer biogeochemical conditions and extend of anthropogenic nitrogen removal. *Water Research*, *123*, 794–801. https://doi.org/10.1016/j.watres.2017.06.048

Tebaldi, C., Hayhoe, K., Arblaster, J. M., & Meehl, G. A. (2006). Going to the extremes: An intercomparison of model-simulated historical and future changes in extreme events. *Climatic Change*, *79*(3-4), 185–211. https://doi.org/10.1007/s10584-006-9051-4

Tian, H. Q., Yang, Q. C., Najjar, R. G., Ren, W., Friedrichs, M. A. M., Hopkinson, C. S., & Pan, S. (2015). Anthropogenic and climatic influences on carbon fluxes from eastern North America to the Atlantic Ocean: A process-based modeling study. *Journal of Geophysical Research: Biogeosciences*, *120*, 757–772. https://doi.org/10.1002/2014JG002760

Tobias, C., & Neubauer, S. C. (2009). In G. M. E. Perillo, et al. (Eds.), *Salt marsh biogeochemistry—An overview in Coastal Wetlands: An integrated ecosystem approach*, (pp. 445–493). The Netherlands: Elsevier.

Turk, D., Zappa, C. J., Meinen, C. S., Christian, J. R., Ho, D. T., Dickson, A. G., & McGillis, W. R. (2010). Rain impacts on CO_2 exchange in the western equatorial Pacific Ocean. *Geophysical Research Letters*, *37*, L23610. https://doi.org/10.1029/2010GL045520

Tzortziou, M., Neale, P., Megonigal, J., Lee Pow, C., & Butterworth, M. (2011). Spatial extent of tidal marsh outwelling in the Rhode River, a subestuary of the Chesapeake Bay. *Marine Ecology Progress Series*, *426*, 41–56. https://doi.org/10.3354/meps09017

Tzortziou, M., Neale, P. J., Osburn, C. L., Megonigal, J. P., Maie, N., & Jaffé, R. (2008). Tidal marshes as a source of optically and chemically distinctive colored dissolved organic matter in the Chesapeake Bay. *Limnology and Oceanography*, *53*(1), 148–159. https://doi.org/10.4319/lo.2008.53.1.0148

Verity, P. G., Yoder, J. A., Stephen Bishop, S., Nelson, J. R., Craven, D. B., Blanton, J. O., et al. (1993). Composition, productivity and nutrient chemistry of a coastal ocean planktonic food web. *Continental Shelf Research*, *13*(7), 741–776. https://doi.org/10.1016/0278-4343(93)90026-T

Vlahos, P., Chen, R. F., & Repeta, D. J. (2002). Dissolved organic carbon in the Mid-Atlantic Bight. *Deep Sea Research Part II: Topical Studies in Oceanography*, *49*(20), 4369–4385. https://doi.org/10.1016/S0967-0645(02)00167-4

Volta, C., Laruelle, G. G., & Regnier, P. (2016). Regional carbon and CO_2 budgets of North Sea tidal estuaries. *Estuarine, Coastal and Shelf Science*, *176*, 76–90. https://doi.org/10.1016/j.ecss.2016.04.007

Wang, Z. A., & Cai, W. J. (2004). Carbon dioxide degassing and inorganic carbon export from a marsh-dominated estuary (the Duplin River): A marsh CO_2 pump. *Limnology and Oceanography*, *49*(2), 341–354. https://doi.org/10.4319/lo.2004.49.2.0341

Wang, W., Johnson, C. G., Takeda, K., & Zafiriou, O. C. (2009). Measuring the photochemical production of carbon dioxide from marine dissolved organic matter by pool isotope exchange. *Environmental Science & Technology*, *43*(22), 8604–8609. https://doi.org/10.1021/es901543e

Wang, Z. A., Kroeger, K. D., Ganju, N. K., Gonneea, M. E., & Chu, S. N. (2016). Intertidal salt marshes as an important source of inorganic carbon to the coastal ocean. *Limnology and Oceanography*, *61*(5), 1916–1931. https://doi.org/10.1002/lno.10347

Wang, Z. A., Wanninkhof, R., Cai, W.-J., Byrne, R. H., Hu, X., Peng, T.-H., & Huang, W.-J. (2013). The marine inorganic carbon system along the Gulf of Mexico and Atlantic coasts of the United States: Insights from a transregional coastal carbon study. *Limnology and Oceanography*, *58*(1), 325–342. https://doi.org/10.4319/lo.2013.58.1.0325

Water Systems Analysis Group (2000). Gulf of Maine watershed information and characterization system database development documentation, Tech. Rep. 00-01. Retrieved from http://www.gm-wics.unh.edu/tech_report00_01/tech_report.html, Accessed December 3, 2016

Weston, N. B., Neubauer, S. C., Velinsky, D. J., & Vile, M. A. (2014). Net ecosystem carbon exchange and the greenhouse gas balance of tidal marshes along an estuarine salinity gradient. *Biogeochemistry*, *120*(1-3), 163–189. https://doi.org/10.1007/s10533-014-9989-7

White, E. M., Kieber, D. J., Sherrard, J., Miller, W. L., & Mopper, K. (2010). Carbon dioxide and carbon monoxide photoproduction quantum yields in the Delaware estuary. *Marine Chemistry*, *118*(1-2), 11–21. https://doi.org/10.1016/j.marchem.2009.10.001

Willey, J. D., Kieber, R. J., Eyman, M. S., & Avery, G. B. Jr. (2000). Rainwater dissolved organic carbon: Concentrations and global flux. *Global Biogeochemical Cycles*, *14*(1), 139–148. https://doi.org/10.1029/1999GB900036

Xiao, Y., & Friedrichs, M. A. M. (2014a). Using biogeochemical data assimilation to assess the relative skill of multiple ecosystem models in the Mid-Atlantic Bight: Effects of increasing the complexity of the planktonic food web. *Biogeosciences*, *11*(11), 3015–3030. https://doi.org/10.5194/bg-11-3015-2014

Xiao, Y., & Friedrichs, M. A. M. (2014b). The assimilation of satellite-derived data into a onedimensional lower trophic level marine ecosystem model. *Journal of Geophysical Research: Oceans*, *119*, 2691–2712. https://doi.org/10.1002/2013JC009433

Xie, L., & Pietrafesa, L. J. (1999). Systemwide modeling of wind and density driven circulation in Croatan-Albemarle-Pamlico estuary system Part I: Model configuration and testing. *Journal of Coastal Research*, *15*, 1163–1177.

Yabro, L. A., & Carlson, P. R. (Eds.) (2011). *Seagrass integrated mapping and monitoring for the State of Florida*, Mapping and Monitoring Rep. 1, 202 pp., Florida Fish and Wildlife Conservation Commission, Fish and Wildlife Research Institute, St. Petersburg, FL.

Yoder, J. (1985). Environmental control of phytoplankton production on the southeastern US continental shelf. In L. P. Atkinson, D. W. Menzel, & K. A. Bush (Eds.), *Oceanography of the Southeastern US Continental Shelf* (pp. 93–103). Washington, DC: American Geophysical Union. https://doi.org/10.1029/CO002p0093

Zimmerman, R., Hill, V., Celebi, B., Jinuntuya, M., Ruble, D., Smith, M., et al. (2017). Experimental impacts of climate warming and ocean carbonation on eelgrass (*Zostera marina* L.). *Marine Ecology Progress Series*, *566*, 1–15. https://doi.org/10.3354/meps12051

Zimmerman, R., Kohrs, D., & Alberte, R. (1996). Top-down impact through a bottom-up mechanism: The effect of limpet grazing on growth, productivity and carbon allocation of *Zostera marina*. *Oecologia*, *107*(4), 560–567. https://doi.org/10.1007/BF00333949

Zimmerman, R., Kohrs, D., Steller, D., & Alberte, R. (1997). Impacts of CO_2 enrichment on productivity and light requirements of eelgrass. *Plant Physiology*, *115*(2), 599–607. https://doi.org/10.1104/pp.115.2.599

Zimmerman, R., Steller, D., Kohrs, D., & Alberte, R. (2001). Top-down impact through a bottom-up mechanism: In situ effects of limpet grazing on growth, light requirements and survival of *Zostera marina* L. (eelgrass). *Marine Ecology Progress Series*, *218*, 127–140. https://doi.org/10.3354/meps218127

Ziolkowski, L. A., & Miller, W. L. (2007). Variability of the apparent quantum efficiency of CO photoproduction in the Gulf of Maine and Northwest Atlantic. *Marine Chemistry*, *105*(3-4), 258–270. https://doi.org/10.1016/j.marchem.2007.02.004

Erratum

In the originally published version of the supporting information, several instances of cell values were incorrect. The following have since been corrected, and this version may be considered the authoritative version of record.

In cell E34, instead of "173.20" it should be "120.2"

In cell G34, instead of "128.97" it should be "120.2"

In cell I34, instead of "125.54" it should be "120.2"

In cell K34, instead of "123.40" it should be "120.2"

In cell E36, instead of "120.99" it should be "71.0"

In cell G36, instead of "79.93" it should be "71.0"

In cell I36, instead of "76.49" it should be "71.0"

In cell K36, instead of "74.31" it should be "71.0"

In cell E38, instead of "262.81" it should be "139.6"

In cell G38, instead of "162.65" it should be "139.6"

In cell I38, instead of "153.87" it should be "139.6"

In cell K38, instead of "148.23" it should be "139.6"

In cell E75, instead of "0.00" it should be "2.3"

In cell G75, instead of "0.00" it should be "10.3"

In cell I75, instead of "0.00" it should be "14.6"

In cell K75, instead of "0.00" it should be "5.6"